Mathematics

https://www.aimspress.com/journal/Math

AIMS Mathematics, 11(9): 30944–30978.
DOI: 10.3934/math.20261225
Received: 22 July 2026
Revised: 02 September 2026
Accepted: 15 September 2026
Published: 21 September 2026

Research article

Stability and Hopf-type bifurcation of a fractional-order delayed SIRS model with behavioral responses driven by positive and negative media information

Xiuduo Liu[1,*] **and Hui Huang**[2]

[1] Department of General Education, Puyang Petrochemical Vocational and Technical College, Puyang 457001, Henan, China

[2] School of Science, Shaoyang University, Shaoyang 422000, Hunan, China

* **Correspondence:** Email: amliuxiuduo@163.com.

Abstract: We established a five-dimensional SIRS epidemic model coupling information–disease dynamics, featuring behavioral responses driven by competitive interactions between positive and negative media information, where the behavioral responses were concretely characterized by an arctangent vaccination willingness function and a fractional linear incidence rate, together with fractional-order memory effects and a behavioral response delay. After proving the well-posedness of the model (existence, uniqueness, nonnegativity, and boundedness of solutions), defining the basic reproduction number $\mathcal{R}_0$, and establishing the existence and uniqueness of the two equilibria, we investigated the local asymptotic stability of the disease-free equilibrium and the endemic equilibrium, as well as the Hopf-type bifurcation of the endemic equilibrium. Specifically, for the disease-free equilibrium, determinant factorization reduced the 5D problem, proving that if the delay-free asymptotic stability condition holds, the presence of the behavioral response delay ($\tau > 0$) does not destabilize the system and no Hopf-type bifurcation occurs. For the endemic equilibrium, using the Sylvester resultant elimination method, a twentieth-degree algebraic criterion provided delay-independent stability conditions and delay-induced Hopf-type bifurcation criteria, yielding an explicit expression for the critical delay. Finally, numerical simulations verified the local asymptotic stability of the disease-free equilibrium, the local asymptotic stability of the endemic equilibrium, and the Hopf-type bifurcation, confirming the theoretical analysis results.

Keywords: fractional-order epidemic model; SIRS model; positive and negative media information; behavioral response delay; stability; Hopf-type bifurcation
Mathematics Subject Classification: 34K37, 34K20, 34K18, 92D30

1. Introduction

Pathogens, population immune status, and behavioral responses jointly determine the epidemiology of infectious diseases. However, these components are often subject to delays and temporal asymmetries, which can give rise to periodic epidemic patterns. COVID-19 is a clear example: Recurrent infection waves have been observed throughout the pandemic. Behavioral response delay played a major role in triggering these complex dynamics [1, 2]. To adequately describe such phenomena, a theoretical model is needed that integrates long-range memory effects (the slow waning of acquired immunity), behavioral delays, and nonlinear information feedback.

Classical integer-order compartment models have laid a solid foundation for infectious disease dynamics [3, 4]. However, in the context of information-driven behavioral interventions, their limitations have become increasingly prominent: First, they cannot capture the gradual waning of immune protection and the cumulative effect of past exposure (memory effects); second, they fail to characterize the destabilization and oscillations induced by the delay from information reception to behavioral execution (time-delay effects); third, it is difficult to describe the nonlinear saturation characteristics of individual behavioral decisions under a competitive information ecology (behavioral feedback).

To overcome the memory and delay limitations identified above, fractional calculus and delay differential equations have been introduced into epidemic modeling. Fractional calculus, with its nonlocal kernel functions and hereditary properties, serves as an ideal tool for characterizing long-range memory effects in biological systems [5, 6]. Among its definitions, the Caputo fractional derivative, which features physically interpretable initial conditions, has been widely introduced into epidemic modeling [7, 8]. Delay differential equations, by incorporating discrete time delays, can endogenously generate Hopf bifurcations and periodic oscillations [9]. Integrating fractional derivatives and discrete time delays into a single system enables the simultaneous capture of memory effects and behavioral delays, and has yielded substantial theoretical advances in epidemic dynamics [10–13], providing methodological support for handling coupled systems with memory and delays, these methodological developments thus provide a natural framework for studying epidemic dynamics under information-driven behavioral interventions.

Building on these methodological advances, several researchers have integrated fractional-order dynamics and time delays into media-influenced epidemic models to capture memory and response lags. For instance, Hu et al. [14] proposed a delayed fractional-order SEIHR-M model and demonstrated that memory effects and behavioral delays can promote oscillatory dynamics under media influence, whereas Wang et al. [15] employed a fractional proportional-derivative control framework to examine the joint effects of time delays and the fractional order on Hopf bifurcation in a model with media coverage and asymptomatic infection. However, these models typically treat information as a single neutral variable and do not account for the competitive nature of the information ecology.

In reality, the information ecology is inherently competitive: Positive science communication and negative rumors co-shape group behavior through dynamic competitive interactions [16–18]. Positive media information (e.g., official public health guidance and authoritative epidemic prevention knowledge) suppresses disease transmission by enhancing public risk perception and protective willingness, whereas negative media information (e.g., rumors, pseudoscientific content, and vaccine misinformation) exacerbates transmission. These two types of information interact competitively within the information ecology and jointly shape population behavioral responses. Researchers have begun to attend to the multidimensional structure and sentiment polarity of information. Recio-Román et al. [19] empirically demonstrated that vaccine hesitancy mediates the influence of media information sources on vaccine uptake. Wang et al. [20] incorporated media sentiment orientation into an SEIR model. Chang et al. [21] characterized the differential propagation effects of positive and negative information in network models, and Alahmadi et al. [22] performed similar characterizations in individual-based models. These works collectively confirm the importance of distinguishing information polarity from different dimensions.

Building on the above developments, we develop a five-dimensional fractional-order delayed SIRS epidemic model that simultaneously incorporates fractional-order memory, behavioral response delay, and competitive positive–negative information effects. Within this unified framework, the model realizes the dual nonlinear regulation of disease transmission by positive and negative information: On the one hand, an arctangent-type vaccination willingness function characterizes the nonlinear saturation feature of individual adoption behaviors under information influence; on the other hand, a fractional linear incidence rate function, through a numerator–denominator antagonistic structure, captures the multiplicative antagonism and diminishing marginal effects of positive and negative information on the effective contact rate. The model employs the Caputo fractional derivative to characterize memory effects, introduces a fixed time delay to represent the time lag from information acquisition to behavioral execution, and sets up two independent compartments for positive information and negative information to describe the dynamic evolution of the information ecology.

In this paper, we will prove the existence, uniqueness, non-negativity, and boundedness of solutions to the model; derive the basic reproduction number $\mathcal{R}_0$, and analyze the existence and uniqueness of the disease-free equilibrium and the endemic equilibrium; focus on revealing, through dimensional reduction of the characteristic equation and the resultant elimination method, the stability switching and Hopf-type bifurcation mechanisms associated with the time delay for both equilibria; and verify the theoretical conclusions through numerical simulations.

2. Model formulation

The system dynamics are described by the following five-dimensional fractional-order delay differential equations:

$$\begin{cases} {}^{C}D_t^{\alpha}S(t) = b - \nu(t-\tau)\dfrac{S(t)I(t)}{N(t)} - \zeta S(t) - c\rho V(t-\tau)S(t) + wR(t), \\ {}^{C}D_t^{\alpha}I(t) = \nu(t-\tau)\dfrac{S(t)I(t)}{N(t)} - (\zeta + d + r)I(t), \\ {}^{C}D_t^{\alpha}R(t) = rI(t) + c\rho V(t-\tau)S(t) - (\zeta + w)R(t), \\ {}^{C}D_t^{\alpha}M_p(t) = \dfrac{\alpha_p I(t)}{1+\beta_p I(t)} + \kappa_p R(t) - \delta_p M_p(t), \\ {}^{C}D_t^{\alpha}M_n(t) = \dfrac{\alpha_n I(t)}{1+\beta_n I(t)} - \delta_n M_n(t), \end{cases} \tag{2.1}$$

where $N(t) = S(t) + I(t) + R(t)$, $c \in (0, 1)$ denotes the vaccine efficacy, ρ is the maximum proportion of susceptible individuals that can be vaccinated per unit time (due to resource constraints), and hence $c\rho$ represents the upper bound of the effective vaccination rate.

In the behavioral response, the vaccination willingness function is defined as an arctangent-type sigmoid function:

$$V(t) = \frac{1}{2} + \frac{1}{\pi}\arctan\left(\frac{\bar{\nu} + \theta_p M_p(t) - \theta_n M_n(t)}{\sigma}\right), \tag{2.2}$$

where $\bar{\nu} \in \mathbb{R}$ is the baseline offset parameter in the absence of information influence, corresponding to the baseline vaccination willingness $V_0 = \frac{1}{2} + \frac{1}{\pi}\arctan(\bar{\nu}/\sigma) \in (0, 1)$; $\sigma > 0$ controls the sensitivity of willingness to changes in information (the smaller σ is, the more dramatic the response, i.e., the steeper the response curve); and $\theta_p, \theta_n > 0$ measure the enhancing effect of positive information and the weakening effect of negative information on vaccination willingness, respectively. The arctangent form naturally ensures that $V \in (0, 1)$ is smooth and differentiable, and is capable of characterizing the nonlinear saturation feature of vaccination willingness as information intensity varies. Although the vaccination willingness at time t is determined by the current information $M_p(t)$ and $M_n(t)$, the actual vaccination behavior takes place after a behavioral response delay τ. Hence, the vaccination term in Eq (2.1) takes the form $c\rho V(t-\tau)S(t)$.

The incidence rate function is defined in a fractional linear form as follows:

$$\nu(t) = \nu_0 \frac{1 + \gamma_n M_n(t)}{1 + \gamma_p M_p(t)}, \tag{2.3}$$

where ν_0 denotes the baseline transmission rate, i.e., the effective contact rate without information influence; $\gamma_p > 0$ and $\gamma_n \geq 0$ quantify the intensity of the impact of positive and negative information on the effective contact rate, respectively. As with the vaccination willingness function $V(t)$, the actual effective contact rate that drives transmission at time t is assumed to depend on the information available at a delayed time $t - \tau$, reflecting the same behavioral response lag. Accordingly, the incidence term in system (2.1) takes the form $\nu(t-\tau)S(t)I(t)/N(t)$, while the function $\nu(\cdot)$ is defined by (2.3) with the instantaneous information variables. This fractional linear form is chosen for three reasons. First, it guarantees a positive lower bound and a finite upper bound for $\nu(t)$ without artificial truncation, provided the information variables are bounded (see Section 4.1). Second, $\partial\nu/\partial M_p < 0$ and $\partial^2\nu/\partial M_p^2 > 0$ imply a diminishing marginal protective effect of positive information, consistent with the behavioral phenomenon of desensitization under information overload. Third, the multiplicative antagonism between the numerator (enhancing transmission via negative information) and the denominator (suppressing it via positive information) captures the opposing impacts of the two information types in a parsimonious manner.

For clarity and to facilitate dimensional consistency checks, all model parameters are summarized in Table 1.

Table 1. Model parameters, biological meanings, units, and admissible ranges.

Parameter	Biological meaning	Unit	Range
α	Order of Caputo derivative	dimensionless	$0 < \alpha < 1$
b	Recruitment rate of susceptible individuals	persons $\cdot$ day$^{-\alpha}$	> 0
ζ	Natural death rate	day$^{-\alpha}$	> 0
d	Disease-induced death rate	day$^{-\alpha}$	> 0
r	Recovery rate	day$^{-\alpha}$	> 0
w	Immunity waning rate	day$^{-\alpha}$	> 0
c	Vaccine efficacy	dimensionless	$(0, 1)$
ρ	Maximum vaccination proportion rate	day$^{-\alpha}$	> 0
ν_0	Baseline transmission rate	day$^{-\alpha}$	> 0
$\gamma_p,\ \gamma_n$	Strength of positive/negative information suppressing/enhancing transmission	dimensionless	$\gamma_p > 0; \gamma_n \geq 0$
$\bar{v}$	Baseline offset of vaccination willingness	dimensionless	$\mathbb{R}$
σ	Sensitivity of willingness to information change	dimensionless	> 0
$\theta_p,\ \theta_n$	Enhancing/weakening effect of positive/negative information on willingness	dimensionless	$\theta_p > 0; \theta_n > 0$
$\alpha_p,\ \alpha_n$	Positive/negative information generation coefficient (from infected)	day$^{-\alpha}$ $\cdot$ person^{-1}	> 0
$\beta_p,\ \beta_n$	Saturation constant of positive/negative information generation	person^{-1}	> 0
κ_p	Contribution coefficient of recovered individuals to positive information	day$^{-\alpha}$ $\cdot$ person^{-1}	> 0
$\delta_p,\ \delta_n$	Decay rate of positive/negative information	day$^{-\alpha}$	> 0
τ	Behavioral response delay	day	> 0

Model (2.1) satisfies the initial conditions $\phi_i(\theta) \geq 0$ $(i = 1, \ldots, 5)$, where $\phi_i(\theta)$ are continuous non-negative functions on $[-\tau, 0]$.

3. Preliminaries

In this paper, we adopt the Caputo fractional derivative, whose definition and properties are given as follows:

Definition 1 (Riemann–Liouville integral [5, 6]). For a function $f \in C([t_0, \infty), \mathbb{R})$, the Riemann–Liouville integral of order $q > 0$ is defined as

$$I^q f(t) = \frac{1}{\Gamma(q)} \int_0^t (t - \zeta)^{q-1} f(\zeta) d\zeta,$$

where $\Gamma(\cdot)$ is the Gamma function.

Definition 2 (Caputo fractional derivative [5, 6])**.** For a function $f \in C^n([t_0, \infty), \mathbb{R})$, the Caputo fractional derivative of order $q \in (n-1, n]$ is defined as

$$ {}_{t_0}^{C}D_t^q f(t) = \frac{1}{\Gamma(n-q)} \int_{t_0}^{t} (t-\zeta)^{n-q-1} f^{(n)}(\zeta)\, d\zeta. $$

In particular, when $0 < q \le 1$,

$$ {}_{t_0}^{C}D_t^q f(t) = \frac{1}{\Gamma(1-q)} \int_{t_0}^{t} \frac{f'(\zeta)}{(t-\zeta)^q}\, d\zeta. $$

Definition 3 (Laplace transform [5, 6])**.** The Laplace transform of the Caputo fractional derivative is given by

$$ L\{{}_{t_0}^{c}D_t^q f(t); s\} = s^q F(s) - \sum_{k=0}^{n-1} s^{q-k-1} f^{(k)}(t_0), $$

where $F(s) = L\{f(t); s\}$ is the Laplace transform of $f(t)$, and $f^{(k)}(t_0)$ denote the initial conditions.

Lemma 1 ([23])**.** *Consider the nonlinear fractional-order time-delay system*

$$ {}^{C}D_t^q \mathbf{x}(t) = \mathbf{f}(\mathbf{x}(t), \mathbf{x}(t-\tau)), \quad 0 < q < 1,\ \tau > 0, \tag{3.1} $$

with $\mathbf{f}(\mathbf{0}, \mathbf{0}) = \mathbf{0}$*. Its linearization around the origin is* $D^q\mathbf{x}(t) = A\mathbf{x}(t) + B\mathbf{x}(t-\tau)$*, where* $A = \frac{\partial \mathbf{f}}{\partial \mathbf{x}(t)}\big|_{\mathbf{0}}$ *and* $B = \frac{\partial \mathbf{f}}{\partial \mathbf{x}(t-\tau)}\big|_{\mathbf{0}}$*. If the following conditions hold:*

(i) All eigenvalues λ *of* $A + B$ *satisfy* $|\arg(\lambda)| > \dfrac{q\pi}{2}$.

(ii) For any $\tau > 0$*, the characteristic equation* $\det(s^q I - A - Be^{-s\tau}) = 0$ *has no purely imaginary roots,*

then the zero solution is locally asymptotically stable.

Lemma 2 ([24])**.** *Let* $0 < \alpha \le 1$ *and consider the autonomous Caputo fractional system*

$$ {}^{C}D^{\alpha} x_i(t) = f_i(x(t)), \qquad i = 1, \ldots, n, \quad t \ge 0, $$

with initial condition $x(0) = x_0 \in \mathbb{R}^n_{\ge 0}$*. Assume that* $f : \mathbb{R}^n \to \mathbb{R}^n$ *is locally Lipschitz continuous and satisfies the classical positivity condition*

$$ \forall\, x \ge 0 \text{ (componentwise)}, \quad x_i = 0 \implies f_i(x) \ge 0 \qquad (i = 1, \ldots, n). $$

Then the unique solution $x(t)$ *remains nonnegative for all* $t \ge 0$*.*

Remark 1. Lemma 2 is stated for autonomous systems, but its proof relies only on the Volterra integral representation and the positivity of the kernel $(t-s)^{\alpha-1}$. If the right-hand side depends explicitly on time, $f_i(t, x)$, and satisfies $x_i = 0 \Rightarrow f_i(t, x) \ge 0$ for all admissible t when the remaining components are non-negative, exactly the same argument yields $x_i(t) \ge 0$. Hence, the lemma also applies to non-autonomous systems ${}^{C}D^{\alpha} x = f(t, x)$ under the same quasi-positivity condition.

Lemma 3 ([25]). *Let $0 < \alpha < 1$ and $u \in C[0,T]$ such that ${}_0^C D_t^\alpha u(t)$ exists on $[0,T]$. If*

$${}_0^C D_t^\alpha u(t) \le -\lambda u(t) + \mu, \qquad t \in [0,T],$$

with $\lambda > 0$, $\mu \ge 0$, and $u(0) \ge 0$, then

$$u(t) \le u(0)E_\alpha(-\lambda t^\alpha) + \frac{\mu}{\lambda}(1 - E_\alpha(-\lambda t^\alpha)) \le \max\{u(0),\ \mu/\lambda\},$$

where E_α is the Mittag-Leffler function.

4. Main results

4.1. Basic properties of the model

In this section, we establish the basic properties of the fractional-order delayed system (2.1) under the given initial conditions.

4.1.1. Existence and uniqueness of solutions

Theorem 1 (Existence and uniqueness of solutions). *Under the assumptions that the parameters are nonnegative and bounded, and $\nu_0, \zeta, b > 0$, system* (2.1) *with the initial condition*

$$X(\theta) = \phi(\theta), \quad \theta \in [-\tau, 0],$$

where $X = (S, I, R, M_p, M_n)$ and $\phi = (\phi_S, \phi_I, \phi_R, \phi_{M_p}, \phi_{M_n}) \in C([-\tau, 0], \mathbb{R}^5_{\ge 0})$ is a given continuous non-negative vector-valued function, possesses a unique solution

$$(S, I, R, M_p, M_n) \in C([-\tau, T];\ \mathbb{R}^5_{\ge 0})$$

on some interval $[0,T]$ with $T > 0$. Moreover, the solution can be extended uniquely to the interval $[0, \infty)$.

Proof. Rewrite system (2.1) as a Caputo fractional functional differential equation

$${}_0^C D_t^\alpha X(t) = F(t, X_t), \qquad X_t(\theta) = X(t+\theta),\ \theta \in [-\tau, 0],$$

where $X = (S, I, R, M_p, M_n)$. We verify that F satisfies the hypotheses of the local existence and uniqueness theorem for such equations (see [26, Theorem 2.8]).

(1) Lipschitz property in the state space. Define the function $h : \mathbb{R}^3_{\ge 0} \to \mathbb{R}$ by

$$h(S, I, R) = \begin{cases} \dfrac{SI}{S+I+R}, & S+I+R > 0, \\ 0, & S+I+R = 0. \end{cases}$$

A direct computation yields

$$\frac{\partial h}{\partial S} = \frac{I(I+R)}{(S+I+R)^2},\ \frac{\partial h}{\partial I} = \frac{S(S+R)}{(S+I+R)^2},\ \frac{\partial h}{\partial R} = -\frac{SI}{(S+I+R)^2},$$

and one readily verifies that

$$\left|\frac{\partial h}{\partial S}\right| \leq 1,\ \left|\frac{\partial h}{\partial I}\right| \leq 1,\ \left|\frac{\partial h}{\partial R}\right| \leq \frac{1}{4}$$

uniformly on $\mathbb{R}^3_{\geq 0} \setminus \{(0,0,0)\}$. Together with the continuity of h at the origin, this implies that h is globally Lipschitz on $\mathbb{R}^3_{\geq 0}$. Consequently, the incidence term $\nu(t-\tau)\,h(S,I,R)$ is locally Lipschitz with respect to X_t because $\nu(t-\tau)$ depends Lipschitz-continuously on $M_n(t-\tau)$, $M_p(t-\tau)$ (the denominator $1+\gamma_p M_p \geq 1$ ensures boundedness) and $V(t-\tau)$ is also Lipschitz in its arguments due to the smoothness of arctan. Thus, on any bounded subset of $C([-\tau,0],\mathbb{R}^5)$, the map $X_t \mapsto F(t,X_t)$ satisfies a Lipschitz condition with respect to the supremum norm.

(2) Continuity in *t*. The functions $\nu(t-\tau)$ and $V(t-\tau)$ depend on t through the history X_t, which is continuous in t by definition. Hence, $F(t,\phi)$ is continuous in t for each fixed ϕ (the C_0-condition).

Therefore, by [26, Theorem 2.8], there exists a unique local solution on some interval $[0,T]$ with $T>0$. Moreover, the uniform boundedness established in Theorem 2 ensures that the solution remains within a compact set, so by the continuation result [26, Theorem 2.11], the solution can be uniquely extended to the interval $[0,\infty)$. □

4.1.2. Non-negativity and boundedness

Theorem 2 (Non-negativity and boundedness)**.** *Under the assumptions of Theorem 1, the solution of system* (2.1) *satisfies:*

(1) $S(t), I(t), R(t), M_p(t), M_n(t) \geq 0$ *for all* $t \geq 0$.
(2) The total population $N(t) = S(t) + I(t) + R(t)$ *is uniformly bounded, and there exist constants* $C_p, C_n > 0$, *such that* $M_p(t) \leq C_p$ *and* $M_n(t) \leq C_n$ *for all* $t \geq 0$.

Proof. **Non-negativity.** We again employ the method of steps and apply the positivity result established in Lemma 2 (see [24]). As noted in Remark 1, this lemma extends directly to non-autonomous systems.

On the first interval $[0,\tau]$, the delayed terms $\nu(t-\tau)$ and $V(t-\tau)$ are known nonnegative continuous functions (because the history functions are nonnegative). Therefore, system (2.1) becomes a non-autonomous fractional ODE ${}^C D^\alpha X = G(t,X)$ with G locally Lipschitz in X. We verify the quasi-positivity condition required by Lemma 2:

If $S = 0$: $\quad G_S(t,X) = b + wR \geq b > 0$.

If $I = 0$: $\quad G_I(t,X) = \nu(t-\tau)\frac{S\cdot 0}{N} - (\zeta + d + r)\cdot 0 = 0$.

If $R = 0$: $\quad G_R(t,X) = rI + c\rho V(t-\tau)S \geq 0$ (since $I, S \geq 0$, $V(t-\tau) \geq 0$).

If $M_p = 0$: $\quad G_{M_p}(t,X) = \frac{\alpha_p I}{1+\beta_p I} + \kappa_p R \geq 0$.

If $M_n = 0$: $\quad G_{M_n}(t,X) = \frac{\alpha_n I}{1+\beta_n I} \geq 0$.

In each case, the right-hand side is nonnegative when the corresponding component is zero and the other components are nonnegative. Hence, by Lemma 2 and Remark 1, the solution satisfies $S(t), I(t), R(t), M_p(t), M_n(t) \geq 0$ for all $t \in [0,\tau]$.

Now assume that nonnegativity holds on $[0,k\tau]$ for some $k \geq 1$. Then on $[k\tau,(k+1)\tau]$, the delayed terms $\nu(t-\tau)$ and $V(t-\tau)$ are evaluated at points $s = t-\tau \leq k\tau$, which are known to be nonnegative.

Consequently, they are nonnegative functions of t on $[k\tau, (k+1)\tau]$. Applying Lemma 2 on this interval yields nonnegativity for the next step. By induction, $S(t), I(t), R(t), M_p(t), M_n(t) \geq 0$ for all $t \geq 0$.
Boundedness. Adding the first three equations of (2.1) gives

$$ {}_0^C D_t^\alpha N(t) = b - \zeta N(t) - dI(t) \leq b - \zeta N(t). $$

Since $N(t)$ is continuous and its fractional derivative exists (equal to the right-hand side, which is continuous), we can apply the comparison Lemma 3 with $\lambda = \zeta > 0$, $\mu = b$, and $u = N$. This yields

$$ N(t) \leq N(0)E_\alpha(-\zeta t^\alpha) + \frac{b}{\zeta}(1 - E_\alpha(-\zeta t^\alpha)) \leq \max\{N(0),\ b/\zeta\} \equiv B_N, \qquad \forall t \geq 0. $$

Hence, $S(t), I(t), R(t) \leq B_N$. We set $B_I = B_R = B_N$.

For M_p, define $g_p(I) = \frac{\alpha_p I}{1+\beta_p I}$. This function satisfies

$$ 0 \leq g_p(I) \leq \begin{cases} \alpha_p/\beta_p, & \beta_p > 0, \\ \alpha_p B_N, & \beta_p = 0. \end{cases} $$

Denote $K_p = \alpha_p/\beta_p$ (if $\beta_p > 0$) or $K_p = \alpha_p B_N$ (if $\beta_p = 0$). Then from the fourth equation,

$$ {}_0^C D_t^\alpha M_p(t) = g_p(I(t)) + \kappa_p R(t) - \delta_p M_p(t) \leq K_p + \kappa_p B_N - \delta_p M_p(t). $$

Again by Lemma 3 with $\lambda = \delta_p$, $\mu = K_p + \kappa_p B_N$, we obtain

$$ M_p(t) \leq \max\{M_p(0),\ (K_p + \kappa_p B_N)/\delta_p\} \equiv C_p. $$

Similarly, for M_n let $g_n(I) = \frac{\alpha_n I}{1+\beta_n I} \leq K_n$, where $K_n = \alpha_n/\beta_n$ (if $\beta_n > 0$) or $K_n = \alpha_n B_N$ (if $\beta_n = 0$). Then

$$ {}_0^C D_t^\alpha M_n(t) = g_n(I(t)) - \delta_n M_n(t) \leq K_n - \delta_n M_n(t), $$

and Lemma 3 gives

$$ M_n(t) \leq \max\{M_n(0),\ K_n/\delta_n\} \equiv C_n. $$

Thus, all variables are uniformly bounded. This completes the proof. □

4.2. *Equilibria and basic reproduction number*

4.2.1. Existence and uniqueness of the disease-free equilibrium

Setting $I = 0$ in (2.1), the fifth equation gives $M_n^0 = 0$. The fourth and third equations yield

$$ M_p^0 = \frac{\kappa_p}{\delta_p} R^0, \qquad R^0 = \frac{c\rho V(M_p^0, 0)}{\zeta + w} S^0. $$

Substituting these into the first equation gives

$$ S^0 = \frac{b(\zeta + w)}{\zeta[\zeta + w + c\rho V(M_p^0, 0)]}. $$

Eliminating S^0 and R^0, the disease-free equilibria are determined by the scalar equation

$$M = H(M) := \frac{b\kappa_p c\rho}{\delta_p \zeta} \frac{V(M,0)}{\zeta + w + c\rho V(M,0)}, \tag{4.1}$$

where

$$V(M,0) = \frac{1}{2} + \frac{1}{\pi} \arctan\left(\frac{\bar{v} + \theta_p M}{\sigma}\right).$$

Since $V(M,0) \in (0,1)$, and $V(M,0)$ is strictly increasing in M, function $H(M)$ is positive, strictly increasing, and bounded above. Therefore,

$$\varphi(M) := H(M) - M$$

satisfies

$$\varphi(0) = H(0) > 0, \qquad \lim_{M\to\infty} \varphi(M) = -\infty.$$

By continuity, φ has at least one zero $M_p^0 \in (0,\infty)$.

To obtain a sufficient condition for uniqueness, we derive a uniform upper bound for $H'(M)$. Let

$$K := \frac{b\kappa_p c\rho}{\delta_p \zeta},$$

and denote the baseline vaccination willingness by

$$V_{00} := V(0,0) = \frac{1}{2} + \frac{1}{\pi} \arctan\left(\frac{\bar{v}}{\sigma}\right) \in (0,1).$$

Since $V(M,0) \geq V_{00} > 0$ and

$$V'(M,0) = \frac{\theta_p}{\pi\sigma} \frac{1}{1 + \left(\frac{\bar{v}+\theta_p M}{\sigma}\right)^2} \leq \frac{\theta_p}{\pi\sigma},$$

it follows that for all $M \geq 0$,

$$H'(M) = K(\zeta + w) \frac{V'(M,0)}{(\zeta + w + c\rho V(M,0))^2} \leq \frac{K(\zeta + w)\theta_p}{(\zeta + w + c\rho V_{00})^2 \pi\sigma} =: L.$$

Thus,

$$\sup_{M\geq 0} H'(M) \leq L.$$

If

$$L = \frac{b\kappa_p c\rho(\zeta + w)\theta_p}{\delta_p \zeta(\zeta + w + c\rho V_{00})^2 \pi\sigma} < 1, \tag{4.2}$$

then $\sup_{M\geq 0} H'(M) < 1$, which implies

$$\varphi'(M) = H'(M) - 1 < 0,$$

for all $M \geq 0$. Therefore, φ is strictly decreasing on $[0,\infty)$. Together with $\varphi(0) > 0$ and $\varphi(+\infty) = -\infty$, this proves that Eq (4.1) has exactly one positive solution M_p^0. Substituting back gives unique positive S^0 and R^0. Consequently, under (4.2), system (2.1) admits a unique disease-free equilibrium

$$E^0 = (S^0, 0, R^0, M_p^0, 0).$$

4.2.2. Basic reproduction number $\mathcal{R}_0$

Applying the next-generation matrix method [3], linearizing the infected compartment I alone at E^0 gives the new infection term $\mathcal{F} = \nu^0 \frac{S^0}{N^0} I$ and the transition term $\mathcal{V} = (\zeta + d + r)I$, where

$$\nu^0 = \frac{\nu_0}{1 + \gamma_p M_p^0}, \quad V^0 = V(M_p^0, 0), \quad N^0 = S^0 + R^0.$$

The corresponding 1×1 matrices are $F = \nu^0 S^0 / N^0$, $V = \zeta + d + r$, and the basic reproduction number is

$$\mathcal{R}_0 = \rho(FV^{-1}) = \frac{\nu^0 S^0}{(\zeta + d + r)N^0}.$$

Using $N^0 = S^0(1 + \frac{c\rho V^0}{\zeta + w}) = S^0 \frac{\zeta + w + c\rho V^0}{\zeta + w}$, we obtain $\frac{S^0}{N^0} = \frac{\zeta + w}{\zeta + w + c\rho V^0}$. Substituting this yields the explicit expression

$$\mathcal{R}_0 = \frac{\nu_0}{(\zeta + d + r)(1 + \gamma_p M_p^0)} \cdot \frac{\zeta + w}{\zeta + w + c\rho V^0}. \tag{4.3}$$

4.2.3. Existence and uniqueness of the endemic equilibrium

For brevity, we introduce the notations

$$m = \zeta + d + r, \qquad \xi = \zeta + w, \qquad \rho_c = c\rho.$$

All equilibria of system (2.1) satisfy the algebraic equations obtained by setting the fractional derivatives to zero. From the equation for the total population

$${}^C D_t^\alpha N(t) = b - \zeta N(t) - dI(t),$$

the steady-state condition yields

$$N(I) = \frac{b - dI}{\zeta}, \qquad 0 \le I < \frac{b}{d}. \tag{4.4}$$

The steady state of M_n is directly solved from the fifth equation in (2.1):

$$M_n(I) = \frac{\alpha_n I}{\delta_n (1 + \beta_n I)}. \tag{4.5}$$

The third equation of (2.1) in steady state gives

$$\rho_c VS + rI = \xi R. \tag{4.6}$$

Using the population identity $N = S + I + R$ to eliminate R, we obtain

$$S = \frac{\xi(N(I) - I) - rI}{\xi + \rho_c V(M_p, M_n(I))}, \tag{4.7}$$

where $V(M_p, M_n(I))$ is given by (2.2) with M_n substituted from (4.5). Equation (4.7) expresses S as a function of M_p for each fixed I.

Substituting (4.7) and the relation $R = N - S - I$ into the steady-state equation for M_p (the fourth equation in (2.1)), we obtain a single equation for M_p:

$$M_p = \mathcal{G}(M_p; I), \tag{4.8}$$

where the map $\mathcal{G}$ is defined by

$$\mathcal{G}(M; I) = \frac{1}{\delta_p}\left(\frac{\alpha_p I}{1 + \beta_p I} + \frac{\kappa_p}{\xi}\Big(rI + \rho_c V(M, M_n(I))S(M; I)\Big)\right), \tag{4.9}$$

with $S(M; I)$ denoting the right-hand side of (4.7) evaluated at $M_p = M$. For later use, we introduce the constant

$$\Gamma = \frac{\kappa_p \rho_c b\,\theta_p}{\delta_p\,\zeta\,\xi\,\pi\sigma}. \tag{4.10}$$

Before establishing the existence and uniqueness of $M_p(I)$, we identify the biologically feasible range of I. Define

$$\Phi(I) := \xi(N(I) - I) - rI = \frac{\xi b}{\zeta} - \left(\frac{\xi d}{\zeta} + \xi + r\right)I.$$

Thus, $\Phi(0) = \xi b/\zeta > 0$ and $\Phi(b/d) = -\frac{(\xi+r)b}{d} < 0$. Hence, there exists a unique

$$I_c \in (0, b/d)$$

such that $\Phi(I_c) = 0$. For $I \in [0, I_c]$, the numerator of S in (4.7) is non-negative, so $S \geq 0$. For $I > I_c$, $S < 0$, which is biologically irrelevant. We therefore restrict the subsequent construction to the feasible interval $I \in [0, I_c]$.

Lemma 4. *Assume* $\Gamma < 1$. *Then for every* $I \in [0, I_c]$, *Eq* (4.8) *admits a unique solution* $M_p = M_p(I)$. *Moreover,* $M_p(I)$ *is continuously differentiable on* $[0, I_c]$.

Proof. We first estimate the partial derivative of $\mathcal{G}$ with respect to M. Differentiating (4.7) with respect to M (keeping I fixed) gives

$$\frac{\partial S}{\partial M} = -\frac{\rho_c\,\partial_M V\,S}{\xi + \rho_c V} \quad \text{with} \quad \partial_M V \equiv \frac{\partial V}{\partial M_p}(M, M_n(I)).$$

Consequently,

$$\frac{\partial}{\partial M}(VS) = \partial_M V \cdot S + V\frac{\partial S}{\partial M} = \frac{\xi\,\partial_M V\,S}{\xi + \rho_c V}.$$

Using this in (4.9), we obtain

$$\frac{\partial \mathcal{G}}{\partial M}(M; I) = \frac{\kappa_p \rho_c}{\delta_p \xi}\,\frac{\xi\,\partial_M V\,S}{\xi + \rho_c V} = \frac{\kappa_p \rho_c\,\partial_M V\,S}{\delta_p(\xi + \rho_c V)}. \tag{4.11}$$

From the definition of V in (2.2), one has $|\partial_M V| \leq \theta_p/(\pi\sigma)$. For $I \in [0, I_c]$, by the definition of I_c, we have $S \geq 0$ and

$$S = \frac{\Phi(I)}{\xi + \rho_c V} \leq \frac{\Phi(I)}{\xi} \leq \frac{\xi N(I)}{\xi} = N(I) \leq \frac{b}{\zeta},$$

since $\Phi(I) \leq \xi N(I)$. Thus, $|S| = S \leq b/\zeta$. Since $\xi + \rho_c V \geq \xi$, we obtain

$$\Big|\frac{\partial \mathcal{G}}{\partial M}(M; I)\Big| \leq \frac{\kappa_p \rho_c}{\delta_p \xi}\,\frac{\theta_p}{\pi\sigma}\,\frac{b}{\zeta} = \Gamma < 1.$$

Thus, $\mathcal{G}(\cdot; I)$ is a contraction uniformly in $I \in [0, I_c]$.

To apply the Banach fixed-point theorem, we construct a compact interval that is invariant under $\mathcal{G}(\cdot; I)$. Set

$$M_{\max} = \frac{1}{\delta_p}\bigg(\frac{\alpha_p b}{d} + \frac{\kappa_p}{\xi}\Big(\frac{rb}{d} + \frac{\rho_c b}{\zeta}\Big)\bigg).$$

For any $M \in [0, M_{\max}]$ and $I \in [0, I_c]$, we have

$$\mathcal{G}(M; I) \leq \frac{1}{\delta_p}\bigg(\frac{\alpha_p I}{1 + \beta_p I} + \frac{\kappa_p}{\xi}\Big(rI + \rho_c \cdot 1 \cdot \frac{b}{\zeta}\Big)\bigg) \leq M_{\max},$$

and clearly $\mathcal{G}(M; I) \geq 0$. Hence, $\mathcal{G}(\cdot; I)$ maps $[0, M_{\max}]$ into itself. Since $[0, M_{\max}]$ is a complete metric space, the Banach fixed-point theorem guarantees a unique fixed point $M_p(I) \in [0, M_{\max}]$, satisfying (4.8).

The continuous differentiability of $M_p(I)$ follows from the implicit function theorem. Indeed, $\mathcal{G}(M, I)$ is continuously differentiable in both variables on $[0, M_{\max}]\times [0, I_c]$. Because $|\partial_M \mathcal{G}| \leq \Gamma < 1$, the derivative $1 - \partial_M \mathcal{G}$ never vanishes. Therefore, $M_p(I)$ is C^1 on $[0, I_c]$. □

With $M_p(I)$ uniquely determined by Lemma 4, we define

$$S(I) = \frac{\xi(N(I) - I) - rI}{\xi + \rho_c V(M_p(I), M_n(I))}, \qquad R(I) = N(I) - S(I) - I,$$

which are continuously differentiable on $[0, I_c]$. On this interval, $S(I) \geq 0$ and $N(I) > 0$.

To close the equilibrium problem, we substitute the functions $S(I)$, $N(I)$, $M_p(I)$, and $M_n(I)$ into the left-hand side of the infected compartment equation. Define the residual function

$$\Psi(I) = \nu(M_p(I), M_n(I))\frac{S(I)}{N(I)} - m, \qquad I \in [0, I_c], \tag{4.12}$$

where $\nu(M_p, M_n)$ is given by (2.3). Then I^* is the infected component of an endemic equilibrium if and only if $\Psi(I^*) = 0$.

At $I = 0$, the functions $M_p(I), S(I), N(I)$ reduce precisely to the disease-free equilibrium values M_p^0, S^0, N^0 (the fixed point at $I = 0$ coincides with the unique DFE established in Section 4.2.1). Using the expression (4.3) for the basic reproduction number, we obtain

$$\Psi(0) = \nu(M_p^0, 0)\frac{S^0}{N^0} - m = m(\mathcal{R}_0 - 1). \tag{4.13}$$

At the right endpoint, $S(I_c) = 0$ implies

$$\Psi(I_c) = -m < 0. \tag{4.14}$$

Remark 2. The strict decrease of $\Psi(I)$ in Theorem 3 is a checkable condition. Differentiating (4.12) gives

$$\Psi'(I) = \left(\frac{\partial \nu}{\partial M_p} M_p'(I) + \frac{\partial \nu}{\partial M_n} M_n'(I)\right) \frac{S(I)}{N(I)} + \nu(M_p(I), M_n(I)) \frac{d}{dI}\left(\frac{S(I)}{N(I)}\right).$$

The sign of the second term is not a priori fixed, because the derivative of $S(I)/N(I)$ depends on the information-dependent denominator. In particular, $S(I)/N(I)$ may not be monotone in I. Nevertheless, a conservative but explicit sufficient condition can be derived as follows:

Let

$$C_0 = \frac{\alpha_n}{\delta_n}.$$

To bound $M_p'(I)$, we use the implicit function theorem. From $M_p(I) = \mathcal{G}(M_p(I); I)$,

$$M_p'(I) = \frac{\partial_I \mathcal{G}(M_p(I); I)}{1 - \partial_M \mathcal{G}(M_p(I); I)}.$$

Differentiating (4.9) with respect to I gives

$$\partial_I \mathcal{G}(M; I) = \frac{1}{\delta_p}\left[\frac{\alpha_p}{(1+\beta_p I)^2} + \frac{\kappa_p}{\xi}\left(r + \rho_c\left(\frac{V A'}{B} + \frac{\xi\, \partial_{M_n} V\, M_n'(I) A}{B^2}\right)\right)\right],$$

where $B = \xi + \rho_c V$ and $A(I) = \xi(N(I) - I) - rI$. Using the estimates

$$|A'| \le a_1 = \frac{\xi d + \zeta(\xi + r)}{\zeta}, \quad A \le \frac{\xi b}{\zeta}, \quad B \ge \xi, \quad |\partial_{M_n} V| \le \frac{\theta_n}{\pi\sigma}, \quad M_n'(I) \le \frac{\alpha_n}{\delta_n},$$

we obtain

$$|\partial_I \mathcal{G}(M; I)| \le \frac{1}{\delta_p}\left[\alpha_p + \frac{\kappa_p}{\xi}\left(r + \rho_c\left(\frac{\xi d + \zeta(\xi + r)}{\zeta\xi} + \frac{\theta_n \alpha_n b}{\pi\sigma\delta_n\zeta}\right)\right)\right] =: C_1.$$

Since $|\partial_M \mathcal{G}| \le \Gamma < 1$, it follows that

$$|M_p'(I)| \le \frac{C_1}{1-\Gamma} =: C_2.$$

Decomposing $\Psi'(I)$ into a negative leading term and several possibly positive terms, and applying the uniform upper bounds C_0 and C_2 (with C_2 derived from C_1 above), we obtain the following conservative sufficient condition. If

$$\gamma_n C_0 + \gamma_p C_2 + \frac{d[\xi d + \zeta(\xi + r)]}{\zeta b(\xi + r)} + \frac{\rho_c}{\xi}\left(\frac{\theta_p C_2 + \theta_n C_0}{\pi\sigma}\right) < \frac{\xi d + \zeta(\xi + r)}{\xi b},$$

then $\Psi'(I) < 0$ for all $I \in (0, I_c)$. Hence, the monotonicity assumption in Theorem 3 is automatically satisfied under this explicit condition.

This condition is sufficient but not necessary, since it is obtained through conservative absolute-value estimates. Moreover, for any fixed parameter set, $\Psi'(I)$ can still be evaluated numerically along the implicitly defined function $M_p(I)$. In all numerical examples presented in this paper, we have verified that $\Psi'(I) < 0$ on $[0, I_c]$.

Theorem 3 (Endemic equilibrium)**.** *Assume* $\Gamma < 1$ *and that* $\Psi(I)$ *is strictly decreasing on* $[0, I_c]$*. Then system* (2.1) *possesses a unique endemic equilibrium* E^* *(with* $I^* > 0$*) if and only if* $\mathcal{R}_0 > 1$.

Proof. If $\mathcal{R}_0 > 1$, then $\Psi(0) > 0$ by (4.13). Since Ψ is continuous and strictly decreasing, and $\Psi(I_c) = -m < 0$, the Intermediate Value Theorem yields a unique $I^* \in (0, I_c)$ such that $\Psi(I^*) = 0$. Substituting I^* into the expressions for $S(I), R(I), M_p(I), M_n(I)$ gives the unique endemic equilibrium E^*.

If $\mathcal{R}_0 \leq 1$, then $\Psi(0) \leq 0$ and the strict decrease of Ψ forces $\Psi(I) < 0$ for all $I \in (0, I_c]$. Hence, no positive root exists. □

4.3. Stability and Hopf-type bifurcation of equilibria

In this section, we investigate the local stability of system (2.1) at the disease-free equilibrium E^0 and the endemic equilibrium E^*, and we discuss the Hopf-type bifurcation condition by taking τ as the bifurcation parameter.

At an arbitrary equilibrium $(S^*, I^*, R^*, M_p^*, M_n^*)$, let $N^* = S^* + I^* + R^*$. Introducing the perturbation variable $\mathbf{X} = (S - S^*, I - I^*, R - R^*, M_p - M_p^*, M_n - M_n^*)^\top$, we write the linearized system as

$$ {}^C D_t^\alpha \mathbf{X}(t) = A\mathbf{X}(t) + B\mathbf{X}(t - \tau), \tag{4.15} $$

where the matrices A and B are given by

$$ A = \begin{pmatrix} a_{11} & a_{12} & a_{13} & 0 & 0 \\ a_{21} & a_{22} & a_{23} & 0 & 0 \\ a_{31} & a_{32} & a_{33} & 0 & 0 \\ 0 & a_{42} & a_{43} & a_{44} & 0 \\ 0 & a_{52} & 0 & 0 & a_{55} \end{pmatrix}, \qquad B = \begin{pmatrix} 0 & 0 & 0 & b_{14} & b_{15} \\ 0 & 0 & 0 & b_{24} & b_{25} \\ 0 & 0 & 0 & b_{34} & b_{35} \\ 0 & 0 & 0 & 0 & 0 \\ 0 & 0 & 0 & 0 & 0 \end{pmatrix}. \tag{4.16} $$

The non-zero entries (with all partial derivatives evaluated at the equilibrium) are:

$$ \begin{aligned} a_{11} &= -\nu^* \tfrac{I^*(I^*+R^*)}{(N^*)^2} - \zeta - c\rho V^*, & a_{12} &= -\nu^* \tfrac{S^*(S^*+R^*)}{(N^*)^2}, \\ a_{13} &= \nu^* \tfrac{S^* I^*}{(N^*)^2} + w, & a_{21} &= \nu^* \tfrac{I^*(I^*+R^*)}{(N^*)^2}, \\ a_{22} &= \nu^* \tfrac{S^*(S^*+R^*)}{(N^*)^2} - (\zeta + d + r), & a_{23} &= -\nu^* \tfrac{S^* I^*}{(N^*)^2}, \\ a_{31} &= c\rho V^*, & a_{32} &= r, \quad a_{33} = -(\zeta + w), \\ a_{42} &= \tfrac{\alpha_p}{(1+\beta_p I^*)^2},\ a_{43} = \kappa_p,\ a_{44} = -\delta_p, & a_{52} &= \tfrac{\alpha_n}{(1+\beta_n I^*)^2},\ a_{55} = -\delta_n, \\ b_{24} &= \tfrac{S^* I^*}{N^*} \partial_{M_p} \nu,\ b_{25} = \tfrac{S^* I^*}{N^*} \partial_{M_n} \nu, & b_{34} &= c\rho S^* \partial_{M_p} V,\ b_{35} = c\rho S^* \partial_{M_n} V, \\ b_{14} &= -b_{24} - b_{34}, & b_{15} &= -b_{25} - b_{35}, \end{aligned} $$

where the partial derivatives are:

$$ \begin{aligned} \left.\frac{\partial \nu}{\partial M_p}\right|_* &= -\frac{\nu_0 \gamma_p (1 + \gamma_n M_n^*)}{(1 + \gamma_p M_p^*)^2} = -\frac{\nu^* \gamma_p}{1 + \gamma_p M_p^*}, & \left.\frac{\partial \nu}{\partial M_n}\right|_* &= \frac{\nu_0 \gamma_n}{1 + \gamma_p M_p^*} = \frac{\nu^* \gamma_n}{1 + \gamma_n M_n^*}, \\ \left.\frac{\partial V}{\partial M_p}\right|_* &= \frac{\theta_p}{\pi\sigma} \cdot \frac{1}{1 + (\frac{\bar{\nu} + \theta_p M_p^* - \theta_n M_n^*}{\sigma})^2}, & \left.\frac{\partial V}{\partial M_n}\right|_* &= -\frac{\theta_n}{\pi\sigma} \cdot \frac{1}{1 + (\frac{\bar{\nu} + \theta_p M_p^* - \theta_n M_n^*}{\sigma})^2}. \end{aligned} $$

4.3.1. Stability and Hopf-type bifurcation of the disease-free equilibrium

At the disease-free equilibrium $E^0 = (S^0, 0, R^0, M_p^0, 0)$, we have $I^* = 0$, which yields $a_{21} = a_{23} = b_{24} = b_{25} = 0$. The characteristic equation of the linearized system can be factorized as

$$\det(s^\alpha I - A - Be^{-s\tau}) = (s^\alpha - (\zeta + d + r)(\mathcal{R}_0 - 1))\,(s^\alpha + \delta_n)\,\Delta(s,\tau) = 0, \tag{4.17}$$

where

$$\Delta(s,\tau) = \det\begin{pmatrix} s^\alpha + \zeta + c\rho V^0 & -w & -b_{14}e^{-s\tau} \\ -c\rho V^0 & s^\alpha + \zeta + w & -b_{34}e^{-s\tau} \\ 0 & -\kappa_p & s^\alpha + \delta_p \end{pmatrix},$$

and $b_{34} = -b_{14} = c\rho S^0 \frac{\partial V}{\partial M_p}\Big|_0$; since $\frac{\partial V}{\partial M_p}\Big|_0 > 0$, we have $b_{34} > 0$.

When $\mathcal{R}_0 < 1$, the equation

$$s^\alpha - (\zeta + d + r)(\mathcal{R}_0 - 1) = 0$$

gives

$$\lambda = s^\alpha = (\zeta + d + r)(\mathcal{R}_0 - 1) < 0,$$

so $|\arg(\lambda)| = \pi > \alpha\pi/2$ ($\alpha \in (0,1)$). Similarly,

$$s^\alpha + \delta_n = 0$$

gives

$$\lambda = s^\alpha = -\delta_n < 0,$$

and again $|\arg(\lambda)| > \alpha\pi/2$. Therefore, the corresponding eigenvalues lie in the fractional-order stability region, and the stability of E^0 is determined solely by $\Delta(s,\tau) = 0$.

We now apply elementary operations to $\Delta(s,\tau)$ to reduce its order. Adding the second row to the first row (which leaves the determinant unchanged) and using $b_{14} + b_{34} = 0$, we obtain

$$\Delta(s,\tau) = \det\begin{pmatrix} s^\alpha + \zeta & s^\alpha + \zeta & 0 \\ -c\rho V^0 & s^\alpha + \zeta + w & -b_{34}e^{-s\tau} \\ 0 & -\kappa_p & s^\alpha + \delta_p \end{pmatrix}.$$

Factoring $s^\alpha + \zeta$ from the first row, then subtracting the first column from the second column (a column operation that does not alter the determinant), and expanding along the first row, we obtain

$$\Delta(s,\tau) = (s^\alpha + \zeta)\,\det\begin{pmatrix} s^\alpha + \zeta + w + c\rho V^0 & -b_{34}e^{-s\tau} \\ -\kappa_p & s^\alpha + \delta_p \end{pmatrix}.$$

Evaluating this 2×2 determinant yields the factorized form

$$\Delta(s,\tau) = (s^\alpha + \zeta)\Big[s^{2\alpha} + A_1 s^\alpha + A_2 - \kappa_p b_{34} e^{-s\tau}\Big], \tag{4.18}$$

where, setting $\beta = \zeta + w + c\rho V^0 > 0$, we have

$$A_1 = \beta + \delta_p > 0, \qquad A_2 = \delta_p \beta > 0. \tag{4.19}$$

For the factor $s^\alpha + \zeta = 0$, setting $\lambda = s^\alpha$ gives $\lambda = -\zeta < 0$, so $|\arg(\lambda)| = \pi > \alpha\pi/2$. Hence, this factor also contributes only stable modes. Consequently, the local stability and possible Hopf-type bifurcation of E^0 are determined by the roots of Eq (4.20).

$$\widetilde{\Delta}(s,\tau) := s^{2\alpha} + A_1 s^\alpha + A_2 - Qe^{-s\tau} = 0, \qquad Q := \kappa_p b_{34} > 0. \tag{4.20}$$

Theorem 4 (Local stability of the disease-free equilibrium)**.** *Assume that $\alpha \in (0,1)$, $\mathcal{R}_0 < 1$, $A_2 > Q$, and the uniqueness condition* (4.2) *holds. Then, for any delay $\tau \geq 0$, the disease-free equilibrium E^0 is locally asymptotically stable, and the system does not undergo a Hopf-type bifurcation at E^0.*

Proof. We first consider the case $\tau = 0$. Then (4.20) reduces to

$$s^{2\alpha} + A_1 s^{\alpha} + (A_2 - Q) = 0.$$

Let $z = s^{\alpha}$. The equation becomes $z^2 + A_1 z + (A_2 - Q) = 0$. Since $A_1 > 0$ and $A_2 > Q$, all roots of this quadratic equation have negative real parts, so $|\arg(z)| > \pi/2 > \alpha\pi/2$. Hence, E^0 is locally asymptotically stable when $\tau = 0$.

For $\tau > 0$, suppose there exists a purely imaginary root $s = i\omega$ ($\omega > 0$). Substituting into (4.20) and taking the modulus yields

$$|(i\omega)^{2\alpha} + A_1(i\omega)^{\alpha} + A_2| = Q. \tag{4.21}$$

Let $u = \omega^{\alpha} > 0$. Using $(i\omega)^{\alpha} = ue^{i\alpha\pi/2}$, we compute the squared modulus:

$$\begin{aligned} U(u) &:= |u^2 e^{i\alpha\pi} + A_1 u e^{i\alpha\pi/2} + A_2|^2 \\ &= u^4 + 2A_1 \cos\frac{\alpha\pi}{2} u^3 + (A_1^2 + 2A_2\cos\alpha\pi)u^2 + 2A_1A_2\cos\frac{\alpha\pi}{2} u + A_2^2. \end{aligned}$$

Consider the difference

$$U(u) - A_2^2 = u^4 + 2A_1 \cos\frac{\alpha\pi}{2} u^3 + (A_1^2 + 2A_2\cos\alpha\pi)u^2 + 2A_1A_2\cos\frac{\alpha\pi}{2} u.$$

Since $\alpha \in (0,1)$, we have $\cos\frac{\alpha\pi}{2} > 0$, so the coefficients of u^4, u^3, and u are all positive. For the u^2 term, using $\cos\alpha\pi \geq -1$ together with $A_1 = \beta + \delta_p$, $A_2 = \delta_p\beta$, we obtain

$$A_1^2 + 2A_2\cos\alpha\pi \geq A_1^2 - 2A_2 = (\beta + \delta_p)^2 - 2\delta_p\beta = \beta^2 + \delta_p^2 > 0.$$

Therefore, all coefficients of the polynomial $U(u) - A_2^2$ are strictly positive. For every $u > 0$, $U(u) - A_2^2 > 0$, i.e., $U(u) > A_2^2$. Hence,

$$|u^2 e^{i\alpha\pi} + A_1 u e^{i\alpha\pi/2} + A_2| > A_2.$$

Condition $A_2 > Q$ then contradicts the modulus equation (4.21). Thus, for $\tau > 0$, (4.20) admits no purely imaginary roots.

In summary, E^0 is stable at $\tau = 0$, and for all $\tau > 0$ no characteristic root can cross the imaginary axis. Hence, the disease-free equilibrium remains locally asymptotically stable for every $\tau \geq 0$. □

Remark 3. The conditions in Theorem 4 ensure that the disease-free equilibrium is stable when $\tau = 0$, and this stability holds for all $\tau > 0$. This implies that under these conditions, delays in people‘s behavioral responses will not undermine the system’s stability or trigger sustained oscillations.

4.3.2. Stability and Hopf-type bifurcation of the endemic equilibrium

At the endemic equilibrium $E^* = (S^*, I^*, R^*, M_p^*, M_n^*)$, the linearized characteristic equation of system (2.1) reads

$$\begin{aligned}\det(s^\alpha I - A - Be^{-s\tau}) &= s^{5\alpha} + d_4 s^{4\alpha} + d_3 s^{3\alpha} + d_2 s^{2\alpha} + d_1 s^\alpha + d_0 \\ &+ (e_3 s^{3\alpha} + e_2 s^{2\alpha} + e_1 s^\alpha + e_0)e^{-s\tau} + (f_1 s^\alpha + f_0)e^{-2s\tau} = 0,\end{aligned} \tag{4.22}$$

where the coefficients d_i $(i = 0, \dots, 4)$, e_i $(i = 0, \dots, 3)$, and f_i $(i = 1, 2)$ are given explicitly in Appendix A.1.

(1) The delay-free case ($\tau = 0$)

When $\tau = 0$, the characteristic equation (4.22) reduces to

$$s^{5\alpha} + k_4 s^{4\alpha} + k_3 s^{3\alpha} + k_2 s^{2\alpha} + k_1 s^\alpha + k_0 = 0, \tag{4.23}$$

where

$$k_4 = d_4, \quad k_3 = d_3 + e_3, \quad k_2 = d_2 + e_2, \quad k_1 = d_1 + e_1 + f_1, \quad k_0 = d_0 + e_0 + f_0.$$

For $0 < \alpha < 1$, let $\lambda = s^\alpha$. Then (4.23) is equivalent to

$$\lambda^5 + k_4\lambda^4 + k_3\lambda^3 + k_2\lambda^2 + k_1\lambda + k_0 = 0,$$

this polynomial is precisely the characteristic polynomial of the matrix $A + B$, so its roots λ are the eigenvalues of $A + B$. If the Routh–Hurwitz conditions (4.24) hold, then all roots λ of this polynomial have negative real parts, i.e.,

$$|\arg(\lambda)| > \frac{\pi}{2},$$

since $0 < \alpha < 1$, we have $\frac{\pi}{2} > \frac{\alpha\pi}{2}$, and therefore

$$|\arg(\lambda)| > \frac{\alpha\pi}{2},$$

and condition (i) of Lemma 1 is satisfied, and consequently E^* is locally asymptotically stable at $\tau = 0$.

Specifically, the Routh–Hurwitz conditions are as follows:

$$\begin{aligned}&k_i > 0 \quad (i = 0, 1, \dots, 4), && H_3 = k_4k_3k_2 + k_4k_0 - k_4^2k_1 - k_2^2 > 0, \\ &H_2 = k_4k_3 - k_2 > 0, && H_4 = (k_4k_3 - k_2)(k_2k_1 - k_3k_0) - (k_4k_1 - k_0)^2 > 0.\end{aligned} \tag{4.24}$$

Under these conditions, all roots of the polynomial in λ have negative real parts, so Lemma 1(i) holds, and E^* is locally asymptotically stable at $\tau = 0$.

(2) The case with delay ($\tau > 0$)

We look for purely imaginary roots $s = i\omega$ $(\omega > 0)$ and set $z = e^{-i\omega\tau}$. The characteristic equation (4.22) can then be rewritten as the following quadratic equation in z:

$$P(\omega)z^2 + E(\omega)z + D(\omega) = 0, \tag{4.25}$$

where

$$\begin{aligned}D(\omega) &= (i\omega)^{5\alpha} + d_4(i\omega)^{4\alpha} + d_3(i\omega)^{3\alpha} + d_2(i\omega)^{2\alpha} + d_1(i\omega)^\alpha + d_0, \\ E(\omega) &= e_3(i\omega)^{3\alpha} + e_2(i\omega)^{2\alpha} + e_1(i\omega)^\alpha + e_0, \\ P(\omega) &= f_1(i\omega)^\alpha + f_0.\end{aligned}$$

Using $(i\omega)^{k\alpha} = \omega^{k\alpha} e^{ik\alpha\pi/2}$ to separate real and imaginary parts, we write

$$D = D_r + iD_i, \quad E = E_r + iE_i, \quad P = P_r + iP_i,$$

with

$$\begin{aligned}
D_r &= \omega^{5\alpha}\cos\frac{5\alpha\pi}{2} + d_4\omega^{4\alpha}\cos(2\alpha\pi) + d_3\omega^{3\alpha}\cos\frac{3\alpha\pi}{2} + d_2\omega^{2\alpha}\cos(\alpha\pi) + d_1\omega^{\alpha}\cos\frac{\alpha\pi}{2} + d_0,\\
D_i &= \omega^{5\alpha}\sin\frac{5\alpha\pi}{2} + d_4\omega^{4\alpha}\sin(2\alpha\pi) + d_3\omega^{3\alpha}\sin\frac{3\alpha\pi}{2} + d_2\omega^{2\alpha}\sin(\alpha\pi) + d_1\omega^{\alpha}\sin\frac{\alpha\pi}{2},\\
E_r &= e_3\omega^{3\alpha}\cos\frac{3\alpha\pi}{2} + e_2\omega^{2\alpha}\cos(\alpha\pi) + e_1\omega^{\alpha}\cos\frac{\alpha\pi}{2} + e_0,\\
E_i &= e_3\omega^{3\alpha}\sin\frac{3\alpha\pi}{2} + e_2\omega^{2\alpha}\sin(\alpha\pi) + e_1\omega^{\alpha}\sin\frac{\alpha\pi}{2},\\
P_r &= f_1\omega^{\alpha}\cos\frac{\alpha\pi}{2} + f_0, \qquad P_i = f_1\omega^{\alpha}\sin\frac{\alpha\pi}{2}.
\end{aligned}$$

Since $|z| = 1$, taking the complex conjugate of (4.25) yields $\overline{D}z^2 + \overline{E}z + \overline{P} = 0$. Eliminating z from the two equations and applying the Sylvester resultant, we obtain

$$\chi(\omega) := (|P|^2 - |D|^2)^2 - \left|P\overline{E} - E\overline{D}\right|^2 = 0, \tag{4.26}$$

where $|D|^2 = D_r^2 + D_i^2$, $|E|^2 = E_r^2 + E_i^2$, $|P|^2 = P_r^2 + P_i^2$. Substituting the expressions of the real and imaginary parts and letting $x = \omega^\alpha$, $\chi(\omega)$ can be reduced to a polynomial in x, whose leading term is x^{20}:

$$\chi(x) = x^{20} + \eta_{19}x^{19} + \cdots + \eta_1 x + \eta_0 = 0, \qquad x > 0. \tag{4.27}$$

The coefficients η_j ($j = 0, \ldots, 19$) are determined by the model parameters and the fractional order α; their explicit expressions are given in Appendix A.2.

It is important to emphasize that (4.26) is only a *necessary* condition for the existence of a purely imaginary root $s = i\omega$. Indeed, the vanishing of the Sylvester resultant guarantees only that the two polynomials

$$P(\omega)z^2 + E(\omega)z + D(\omega) \quad \text{and} \quad \overline{D}(\omega)z^2 + \overline{E}(\omega)z + \overline{P}(\omega)$$

have a common root, but this common root may not lie on the unit circle. Therefore, a positive real root x_j of (4.27) does not automatically yield an admissible $z = e^{-i\omega_j\tau}$ with $|z| = 1$.

Theorem 5 (Stability of the endemic equilibrium)**.** *Let $\alpha \in (0, 1)$. Assume that the following conditions hold simultaneously:*

(1) The conditions of Theorem 3 hold (i.e., E^* exists and is unique).
(2) Condition (4.24) holds (so that E^* is locally asymptotically stable when $\tau = 0$).
(3) The polynomial $\chi(x)$ has no real root on $(0, +\infty)$.

Then the endemic equilibrium E^* remains locally asymptotically stable for any delay $\tau > 0$.

(3) Hopf-type bifurcation analysis

Since the Hopf bifurcation theory for fractional-order delay systems is under development, and a completely rigorous general theoretical proof of the existence of periodic solutions after bifurcation remains an open problem, the Hopf bifurcation analysis in this paper adopts a semi-analytical and semi-numerical approach.

In this framework, we adopt the widely used criteria proposed by Xiao et al. [9] as the analytical basis for the occurrence of Hopf-type bifurcation. Throughout this section, the term "Hopf-type bifurcation" is used in the sense of this criterion. Specifically, Xiao et al. considered the following n-dimensional fractional-order system with delay:

$$ {}^{C}\mathcal{D}_t^q x_j(t) = f_j(\mathbf{x}(t), \mathbf{x}(t-\tau); \tau), \quad j = 1, \dots, n, \ 0 < q < 1, \ \tau \geq 0. \tag{4.28} $$

System (4.28) undergoes a Hopf bifurcation at the equilibrium $\mathbf{x}^*$ when $\tau = \tau_0$, if the following conditions hold:

(i) For $\tau = 0$, all eigenvalues of the coefficient matrix of the linearized system satisfy $|\arg(\lambda)| > q\pi/2$.
(ii) At $\tau = \tau_0$, the characteristic equation $\det(s^q I - A - Be^{-s\tau}) = 0$ has a pair of purely imaginary roots $\pm i\omega_0$.
(iii) The transversality condition $\mathrm{Re}\left[\dfrac{\mathrm{d}s}{\mathrm{d}\tau}\right]_{\tau=\tau_0, s=i\omega_0} > 0$ is satisfied.

We now apply the above criterion to our model. As shown in the discussion of Section 4.3.2 for the case $\tau = 0$, if condition (4.24) holds, then E^* is locally asymptotically stable when $\tau = 0$, which precisely corresponds to condition (i) in the above criterion.

Next, we examine condition (ii) for the occurrence of Hopf-type bifurcation. In solving for purely imaginary roots, the equation $\chi(\omega) = 0$ is only a *necessary* condition for the existence of purely imaginary roots of the characteristic equation (4.22). Therefore, to verify condition (ii), one must further check whether the corresponding quadratic equation (4.25) possesses a root of modulus one.

If the constant term of (4.27) satisfies $\eta_0 < 0$, then $\chi(0) = \eta_0 < 0$ and $\lim_{x\to+\infty} \chi(x) = +\infty$, so the polynomial $\chi(x)$ admits at least one positive real root. More generally, let

$$ \mathcal{X} = \{\, x_j > 0 : \chi(x_j) = 0 \,\} $$

be the set of all positive real roots of χ. For each $x_j \in \mathcal{X}$, set

$$ \omega_j = x_j^{1/\alpha} > 0 $$

and substitute $s = i\omega_j$ into the characteristic equation. This is equivalent to solving the quadratic equation

$$ P(\omega_j)z^2 + E(\omega_j)z + D(\omega_j) = 0. $$

Let $z_{j,1}$ and $z_{j,2}$ be its two roots. Define the set of *admissible pairs* by

$$ \Lambda = \{\, (\omega_j, z_{j,\ell}) : x_j \in \mathcal{X}, \ \ell = 1, 2, \ |z_{j,\ell}| = 1 \,\}. $$

If $\Lambda \neq \emptyset$, then for each admissible pair $(\omega_j, z_{j,\ell}) \in \Lambda$, we may write

$$ z_{j,\ell} = e^{-i\theta_{j,\ell}}, \qquad \theta_{j,\ell} \in [0, 2\pi), $$

and the corresponding critical delays are

$$ \tau_{j,\ell,k} = \frac{\theta_{j,\ell} + 2k\pi}{\omega_j}, \qquad k = 0, 1, 2, \dots. $$

The first possible stability switch is obtained by taking the minimum over all admissible positive delays:

$$\tau_c = \min_{\substack{(\omega_j, z_{j,\ell}) \in \Lambda \\ k \geq 0}} \{\tau_{j,\ell,k} > 0\}. \tag{4.29}$$

Let (ω_c, z_c) be the unique admissible pair attaining the above minimum, so that

$$z_c = e^{-i\theta_c}, \qquad \theta_c \in [0, 2\pi),$$

and

$$\tau_c = \frac{\theta_c + 2k_c\pi}{\omega_c}$$

for some integer $k_c \geq 0$.

Finally, we impose the transversality condition. Regard s as a function of τ and differentiate the characteristic equation (4.22) implicitly to obtain $\frac{\mathrm{d}s}{\mathrm{d}\tau}$. When $s = i\omega_c$ and $\tau = \tau_c$, suppose that

$$\mathrm{Re}\left[\frac{\mathrm{d}s}{\mathrm{d}\tau}\right]\Bigg|_{s=i\omega_c,\, \tau=\tau_c} > 0. \tag{4.30}$$

Then condition (iii) holds. Note that the existence of the derivative $\frac{\mathrm{d}s}{\mathrm{d}\tau}$ in (4.30) implies that $\frac{\partial}{\partial s}\det(s^\alpha I - A - Be^{-s\tau})\Big|_{s=i\omega_c,\ \tau=\tau_c} \neq 0$ by the implicit function theorem, and hence the purely imaginary roots $\pm i\omega_c$ are simple.

In summary, we obtain the following theorem.

Theorem 6 (Hopf-type bifurcation of the endemic equilibrium)**.** *Let $\alpha \in (0, 1)$. Assume that the following conditions hold simultaneously:*

(1) The conditions of Theorem 3 hold (i.e., E^* exists and is unique).
(2) Condition (4.24) *holds, so that E^* is locally asymptotically stable when $\tau = 0$.*
(3) $\Lambda \neq \emptyset$, and the minimal positive critical delay τ_c is determined by a unique $\omega_c > 0$ via (4.29).
(4) The transversality condition (4.30) *holds at (ω_c, τ_c).*

Then, E^* is locally asymptotically stable for all $\tau \in [0, \tau_c)$, and the system undergoes a Hopf-type bifurcation at E^* as τ passes through τ_c.

Remark 4. Theorems 5 and 6 describe the local dynamics around the endemic equilibrium E^*. Under the conditions of Theorem 5, the endemic equilibrium is locally asymptotically stable; in this case, the behavioral response delay cannot trigger a Hopf-type bifurcation or oscillatory behavior around the equilibrium. On the other hand, when the conditions of Theorem 6 are satisfied, there exists a critical delay $\tau_c > 0$ such that E^* remains locally asymptotically stable for $\tau \in [0, \tau_c)$, and a Hopf-type bifurcation occurs at $\tau = \tau_c$. We will further verify and demonstrate the above dynamical behaviors through numerical examples in the numerical simulation section.

5. Numerical simulations

In this section, numerical simulations are performed to verify the theoretical results. All simulations are based on MATLAB, using the Adams–Bashforth–Moulton predictor-corrector algorithm [27]. For every numerical simulation example considered below, the parameter values are selected through a Monte Carlo sampling procedure within the admissible ranges specified in Table 1. In each case, candidate parameter sets are generated randomly and then screened according to the corresponding theoretical conditions established in the preceding sections. All parameter sets obtained in this way are representative configurations designed to illustrate the mathematical conditions and dynamical scenarios derived in the theoretical analysis, rather than being calibrated from epidemiological data.

5.1. Stability of the disease-free equilibrium

The parameters are chosen as follows:

$b = 0.154668455$, $\zeta = 3.11276 \times 10^{-5}$, $d = 0.001820759$, $r = 0.311522005$, $w = 0.006540418$, $c = 0.914055806$, $\rho = 0.004150002$, $\bar{\nu} = -1.893804497$, $\sigma = 1.631706099$, $\theta_p = 0.912860953$, $\theta_n = 2.73487166$, $\alpha_p = 0.217440261$, $\alpha_n = 0.166237291$, $\beta_p = 0.079979228$, $\beta_n = 0.10632897$, $\kappa_p = 5.30653 \times 10^{-5}$, $\delta_p = 0.382025912$, $\delta_n = 0.331762137$, $\nu_0 = 0.437891367$, $\gamma_p = 4.661767789$, $\gamma_n = 3.696530826$, $\alpha = 0.95$.

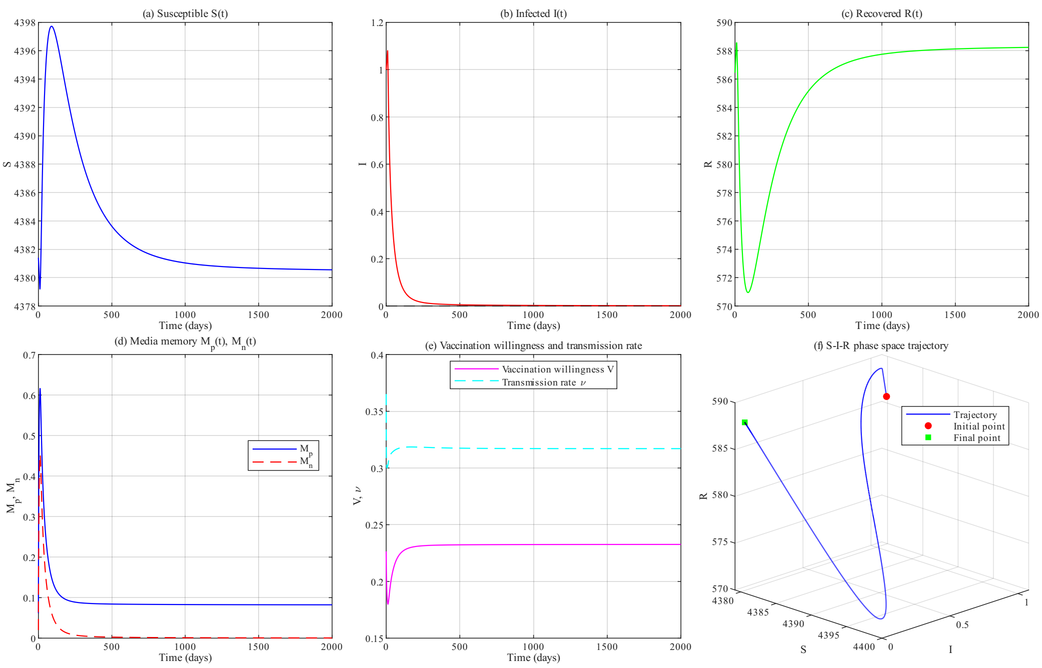

Figure 1. State trajectories when the disease-free equilibrium is locally asymptotically stable ($\tau = 10$).

For this parameter set, direct calculation yields

$$L = \frac{b\kappa_p c\rho(\zeta + w)\theta_p}{\delta_p \zeta(\zeta + w + c\rho V_{00})^2 \pi\sigma} = 0.055496452 < 1,$$

which satisfies the first condition of Theorem 4, guaranteeing the existence and uniqueness of the disease-free equilibrium. The disease-free equilibrium is calculated as: $S^0 = 4380.400955$, $I^0 = 0$, $R^0 = 588.4476742$, $M_p^0 = 0.081738285$, $M_n^0 = 0$, $V^0 = 0.232723615$, and the basic reproduction number $\mathcal{R}_0 = 0.891977443 < 1, A2 = 0.0019728563 > Q = 0.0010263368$. That is, Theorem 4 is satisfied. Taking the initial condition $(S^0+1, 1, R^0-2, M_p^0-0.02, 0.02)$ and the delay $\tau = 10$, as shown in Figure 1, the system converges to the disease-free equilibrium.

5.2. *Stability of the endemic equilibrium and Hopf-type bifurcation*

5.2.1. Local stability of the endemic equilibrium

The parameters are chosen as:

$$\begin{aligned}
&b = 0.127941362,\ \zeta = 4.54334\times10^{-5}, d = 0.003138141,\ \ r = 0.213262544,\ \ w = 0.009684088,\\
&c = 0.75093639,\ \ \rho = 0.008355527,\ \ \bar{v} = -1.833673949, \sigma = 1.628162409,\ \theta_p = 1.484519303,\\
&\theta_n = 2.927069562, \alpha_p = 0.219045566,\ \alpha_n = 0.173613855, \beta_p = 0.187983688, \beta_n = 0.154232674,\\
&\kappa_p = 0.000270977, \delta_p = 0.175398899,\ \delta_n = 0.280793805,\ \nu_0 = 1.569825824, \gamma_p = 1.158302728,\\
&\gamma_n = 0.303383105, \alpha = 0.95.
\end{aligned}$$

We obtain $\Gamma = 0.814264 < 1$, and the function $\Psi(I)$ in Eq (4.12) is strictly decreasing (see Figure 2(a)). The basic reproduction number $\mathcal{R}_0 = 2.807338429 > 1$, and a unique endemic equilibrium exists: $S^* = 833.7788938$, $I^* = 20.06176109$, $R^* = 576.4887285$, $M_p^* = 6.14162205$, $M_n^* = 3.029696198$, $V^* = 0.254330918$, $v^* = 0.371308563$. $k_4 = 0.472771414$, $k_3 = 0.056626466$, $k_2 = 0.001695869$, $k_1 = 6.74022\times10^{-5}$, $k_0 = 4.9195\times10^{-9}$, $H_2 = 0.025075505$, $H_3 = 2.74619\times10^{-5}$, $H_4 = 1.84416\times10^{-9}$. The polynomial Eq (18) is given by

$$\begin{aligned}
\chi(x) = x^{20} &+ 0.148372871\,x^{19} + 0.223453059\,x^{18} + 0.023511504\,x^{17} + 0.016840312\,x^{16}\\
&+ 0.00112728\,x^{15} + 0.000485405\,x^{14} + 1.54457\times10^{-5}\,x^{13} + 3.83322\times10^{-6}\,x^{12}\\
&- 3.42916\times10^{-8}\,x^{11} - 2.06297\times10^{-8}\,x^{10} + 7.96966\times10^{-11}\,x^{9}\\
&+ 3.78142\times10^{-11}\,x^{8} - 1.16588\times10^{-13}\,x^{7} - 3.13208\times10^{-14}\,x^{6}\\
&+ 7.57705\times10^{-17}\,x^{5} + 1.05082\times10^{-17}\,x^{4} + 3.01395\times10^{-22}\,x^{3}\\
&+ 1.72045\times10^{-25}\,x^{2} + 2.42638\times10^{-30}\,x + 6.84453\times10^{-34}.
\end{aligned}$$

To verify the absence of positive real roots for the 20th-degree characteristic polynomial $\chi(x)$, we apply Sturm's theorem via Maple to rigorously confirm that no positive real roots exist. This conclusion is further supported by numerical computation of all roots with high precision using the MATLAB routine `roots`, which yields no positive real roots, and by direct evaluation on a fine grid over $(0,\infty)$, which shows $\min_{x>0}\chi(x) > 0$. The conditions of Theorem 5 are satisfied. Taking the delay $\tau = 10$ and the initial condition $(S^*+2,\ I^*-1,\ R^*-1,\ M_p^*+0.5,\ M_n^*+0.5)$, the system converges to the endemic equilibrium (Figure 3).

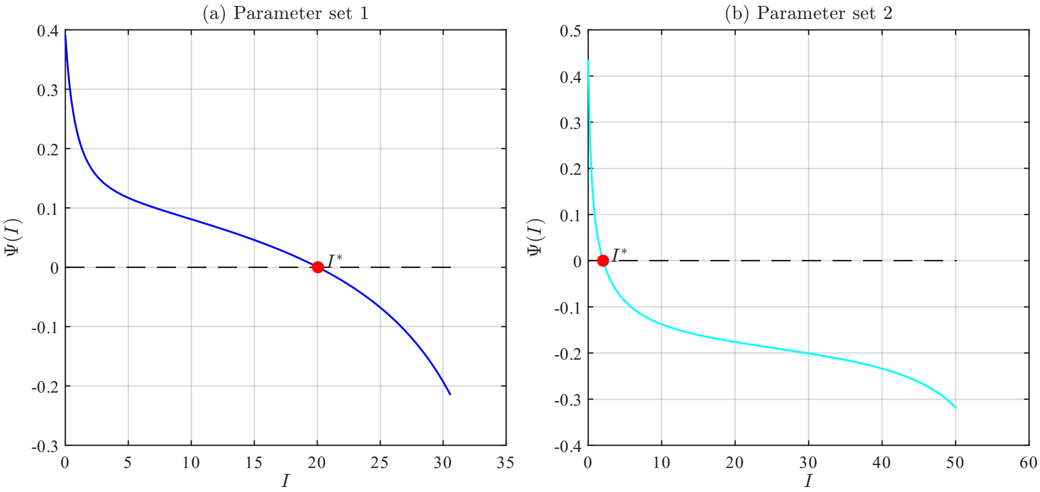

Figure 2. Monotonicity of the residual function $\Psi(I)$.

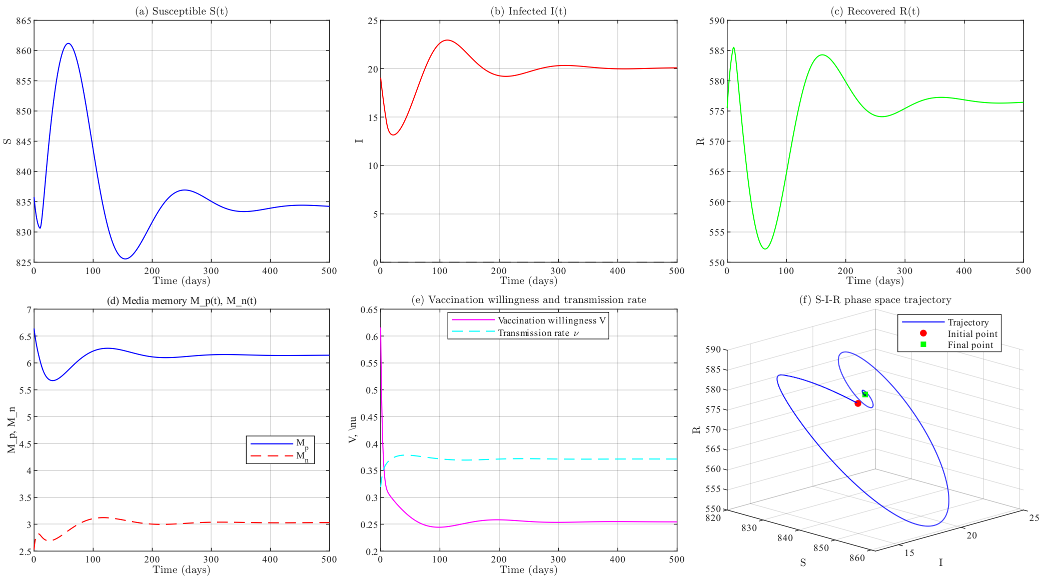

Figure 3. State trajectories when the endemic equilibrium is locally asymptotically stable ($\tau = 10$).

5.2.2. Hopf-type bifurcation at the endemic equilibrium.

The parameters are chosen as:

$b = 0.229780568$, $\zeta = 2.96445 \times 10^{-5}$, $d = 0.003819482$, $r = 0.31644436$, $w = 0.012780409$, $c = 0.781864001$, $\rho = 0.013665765$, $\bar{\nu} = -0.988540658$, $\sigma = 4.166414522$, $\theta_p = 0.843607942$, $\theta_n = 1.672453384$, $\alpha_p = 0.195247027$, $\alpha_n = 0.289201821$, $\beta_p = 0.084647185$, $\beta_n = 0.169460193$, $\kappa_p = 1.77366 \times 10^{-5}$, $\delta_p = 0.105310986$, $\delta_n = 0.444079049$, $\nu_0 = 1.724510465$, $\gamma_p = 1.862238882$, $\gamma_n = 1.096799854$, $\alpha = 0.95$.

We obtain $\Gamma = 0.070179 < 1$, and $\Psi(I)$ in Eq (4.12) is strictly decreasing (Figure 2(b)). The basic reproduction number $\mathcal{R}_0 = 2.36 > 1$, and the unique endemic equilibrium is

$S^* = 5156.203060501674372$, $I^* = 2.022473748851967$, $R^* = 2332.397209286632460$, $M_p^* = 3.594400965672546$, $M_n^* = 0.980923932981140$, $V^* = 0.530706557182485$. For the chosen parameter set, the twentieth-degree resultant polynomial $\chi(x) = x^{20} + \eta_{19}x^{19} + \cdots + \eta_1 x + \eta_0$ is solved numerically using MATLAB's `roots` function, which computes all complex roots via the companion matrix eigenvalue method. Only roots with $|\operatorname{Im}(x_j)| < 10^{-8}$ and $\operatorname{Re}(x_j) > 10^{-6}$ are retained as positive real roots; those with residual $|\chi(x_j)| < 10^{-8}$ are accepted to eliminate spurious roots caused by round-off, and numerically repeated roots (difference $< 10^{-6}$) are merged. The remaining roots x_j are converted to candidate frequencies $\omega_j = x_j^{1/\alpha}$, and for each ω_j the quadratic equation $P(\omega_j)z^2 + E(\omega_j)z + D(\omega_j) = 0$ is solved, retaining only roots satisfying $\left||z| - 1\right| < 10^{-8}$ as admissible roots with $|z| = 1$.

In this case, the above filtering produces only one frequency

$$\omega_c = 0.0672841444448459,$$

which yields the critical delay

$$\tau_c = 4.08889440332154.$$

Furthermore, direct evaluation of the characteristic equation at the critical pair gives

$$|F(i\omega_c, \tau_c)| = \left|\det(s^\alpha I - A - Be^{-s\tau})\Big|_{s=i\omega_c,\, \tau=\tau_c}\right| = 1.6979 \times 10^{-15},$$

which is of the order of machine precision, confirming the correctness of the computed critical pair (ω_c, τ_c).

Since no other frequency remains after the filtering steps, the uniqueness of the purely imaginary root pair at $\tau = \tau_c$ is automatically ensured. If multiple frequencies had been obtained, one should compute the corresponding time delays for all frequencies, select the smallest positive delay as the critical delay, and then substitute all frequencies into the characteristic equation evaluated at that critical delay to verify the uniqueness of the purely imaginary root pair on the stability boundary.

The transversality condition is numerically verified:

$$\operatorname{Re}\left[\frac{\mathrm{d}s}{\mathrm{d}\tau}\right]\Bigg|_{s=i\omega_c,\, \tau=\tau_c} = 0.00175475567214898 > 0.$$

Therefore, all hypotheses of Theorem 6 are satisfied. Taking the initial condition ($S^* + 2$, $I^* - 0.2$, $R^* - 1.8$, $M_p^* + 0.2$, $M_n^* + 0.1$), the numerical simulations are performed using the fractional Adams–Bashforth–Moulton predictor–corrector method. In each time step, the correction is repeated until the maximum absolute difference between two successive corrections is less than the prescribed tolerance tol $= 10^{-12}$, with a maximum of 20 iterations per step. The delayed terms $v(t - \tau)$ and $V(t - \tau)$ are evaluated exactly at the corresponding grid points, since the time step sizes are chosen such that τ/h is an integer, thereby avoiding interpolation errors. Convergence with respect to the temporal resolution is verified by comparing solutions obtained with three step sizes. For the oscillatory case $\tau = 4.14 > \tau_c$, the main run uses $h = 0.0414$, and the computation is repeated with $h = 0.0207$ and $h = 0.01$. Taking the solution with $h = 0.01$ as a reference, the maximum absolute error of $I(t)$ over the last 1000 days is 2.87×10^{-5} for $h = 0.0414$ and 6.71×10^{-6} for $h = 0.0207$, which are less than 0.004% and 0.001% of the oscillation amplitude of $I(t)$, respectively. For the other state variables, the maximum absolute errors are also less than 0.004% of their corresponding amplitudes for $h = 0.0414$, and less than 0.001% for $h = 0.0207$, further confirming that the numerical solution has converged with respect to the temporal resolution. Under these settings, the system undergoes a Hopf-type bifurcation, and the numerical simulations exhibit periodic oscillations(see Figure 4b). Using the same method with fixed step size $h = 0.05$, for $\tau = 3.5 < \tau_c$, the system converges to the endemic equilibrium (see Figure 4a). Moreover, by comparing the trajectories for $\tau = 3.8$ and 4.05, we observe that when $\tau < \tau_c$, the smaller the value of τ, the faster the convergence (see Figure 4a).

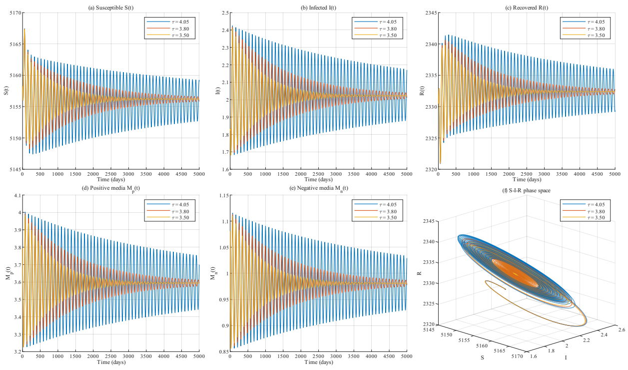

(a) $\tau = 3.5, 3.8, 4.05 < \tau_c$: asymptotically stable.

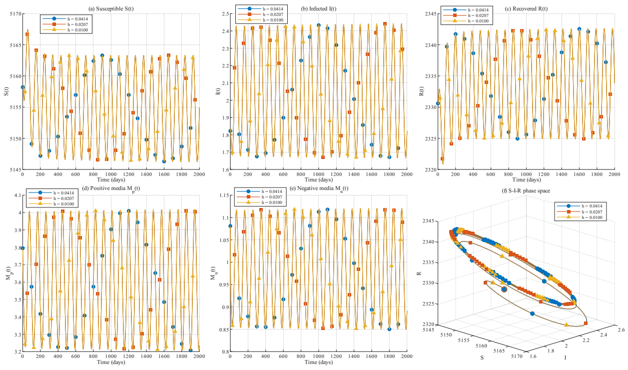

(b) $\tau = 4.14 > \tau_c$: Hopf-type bifurcation.

Figure 4. Delay-induced Hopf-type bifurcation trajectories at the endemic equilibrium.

To further validate the theoretically derived Hopf-type bifurcation threshold, we perform a numerical spectral analysis by tracking the rightmost characteristic root of the linearized fractional-order delay system. Let $s_{\max}$ denote the rightmost characteristic root. The local stability of the system is determined by its real part: The equilibrium is asymptotically stable when $\Re(s_{\max}) < 0$, unstable when $\Re(s_{\max}) > 0$, and a Hopf-type bifurcation occurs when $\Re(s_{\max}) = 0$. Using a continuation method combined with the Newton-type solver (the `fsolve` function in MATLAB), we trace the evolution of $s_{\max}$ as a function of the delay τ over the interval $\tau \in [4.0, 4.2]$. When the real parts at adjacent grid points exhibit opposite signs, the zero-crossing point where $\Re(s_{\max}) = 0$ is precisely located via linear interpolation. As shown in Figure 5, the real part of $s_{\max}$ crosses the imaginary axis smoothly as τ increases. The numerically determined zero-crossing point is

$$\tau_c^{\text{num}} = 4.0888945480.$$

This value is in excellent agreement with the theoretically predicted critical delay

$$\tau_c^{\text{theo}} = 4.0888944033,$$

yielding an absolute error of 1.45×10^{-7} and a relative error of 3.54×10^{-8}. This result numerically confirms the accuracy of the theoretical derivation from the perspective of numerical spectra while demonstrating the reliability of the numerical implementation.

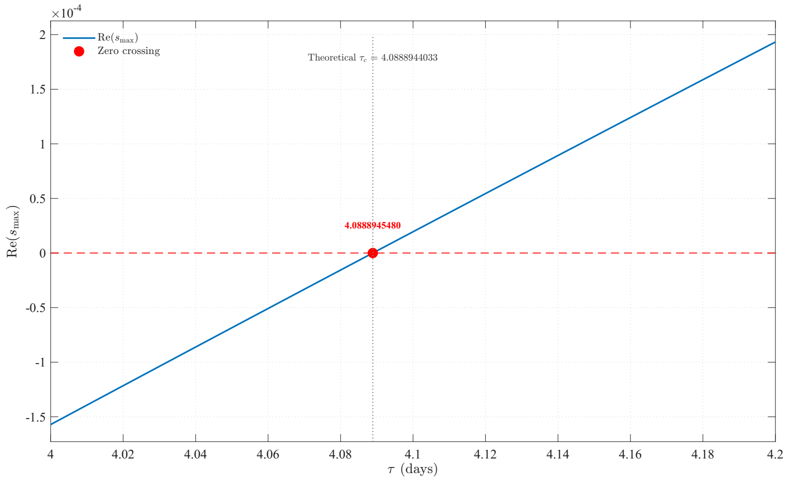

Figure 5. Numerical tracking of the rightmost characteristic root $s_{\max}$.

The fractional order α affects the Hopf-type bifurcation threshold through two mechanisms. First, it modifies the stability sector $|\arg(\lambda)| > \alpha\pi/2$ for the delay-free system, so that a smaller α enlarges the stable region and tends to delay or suppress the onset of oscillations. Second, it enters the characteristic equation through the term s^α, thereby shifting the critical pair (ω_c, τ_c). Numerical experiments show that as α increases from 0.9 to 0.99, the critical delay τ_c decreases monotonically (see Figure (6)).

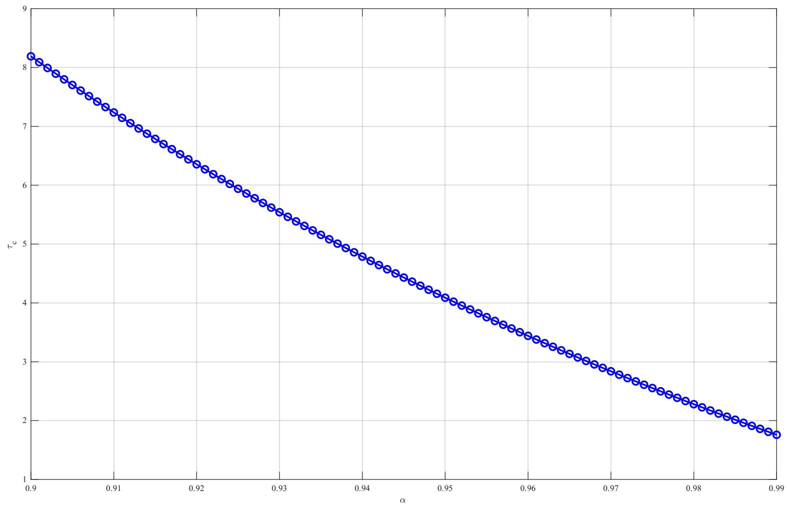

Figure 6. Critical delay τ_c versus α.

6. Conclusions

In this study, we formulate a five-dimensional fractional-order delayed SIRS epidemic model, integrating fractional-order memory effects, behavioral response delays, and the competitive regulation of positive and negative information within a unified framework.

Through rigorous dynamical analysis, two distinct stability scenarios are revealed. Under the premise that the corresponding stability conditions hold in the absence of behavioral response delay ($\tau = 0$), the disease-free equilibrium remains locally asymptotically stable for any behavioral response delay, indicating that behavioral response delay does not undermine the local asymptotic stability of the disease-free equilibrium. For the endemic equilibrium, the system exhibits two types of dynamical behavior: delay-independent stability and delay-induced Hopf-type bifurcation. In the case of delay-induced Hopf-type bifurcation, the existence of a critical delay τ_c suggests that excessively long behavioral response delays can disrupt the feedback regulation of behavioral variables by positive and negative information, preventing the system from converging to an equilibrium and inducing oscillations.

Methodologically, the Sylvester resultant elimination method provides an effective tool for bifurcation analysis of high-dimensional fractional-order delay systems. In future work, researchers may further incorporate state-dependent delays, stochastic information perturbations, and spatial heterogeneity to extend the model's capacity for characterizing complex real-world scenarios.

Author contributions

Xiuduo Liu: Conceptualization, Data curation, Formal analysis, Investigation, Methodology, Software, Validation, Visualization, Writing – original draft; Hui Huang: Writing – review & editing. All authors have read and approved the final version of the manuscript for publication.

Use of Generative-AI tools declaration

The authors declare they have not used Artificial Intelligence (AI) tools in the creation of this article.

Acknowledgments

The authors would like to thank the Key Scientific Research Project of Higher Education of Henan Province (Grant No. 26A110015) for supporting this work.

Conflict of interest

The authors declare no conflicts of interest in this paper.

References

1. A. d'Onofrio, P. Manfredi, Information-related changes in contact patterns may trigger oscillations in the endemic prevalence of infectious diseases, *J. Theor. Biol.*, **256** (2009), 473–478. https://doi.org/10.1016/j.jtbi.2008.10.005
2. C. Maji, F. Al Basir, D. Mukherjee, K. S. Nisar, C. Ravichandran, COVID-19 propagation and the usefulness of awareness-based control measures: a mathematical model with delay, *AIMS Math.*, **7** (2022), 12091–12105. https://doi.org/10.3934/math.2022672
3. P. van den Driessche, J. Watmough, Reproduction numbers and sub-threshold endemic equilibria for compartmental models of disease transmission, *Math. Biosci.*, **180** (2002), 29–48. https://doi.org/10.1016/S0025-5564(02)00108-6

4. J. Cui, Y. Sun, H. Zhu, The impact of media on the control of infectious diseases, *J. Dyn. Differ. Equ.*, **20** (2008), 31–53. https://doi.org/10.1007/s10884-007-9075-0

5. I. Podlubny, *Fractional differential equations*, Mathematics in Science and Engineering, New York: Academic Press, 1999. https://doi.org/10.1016/s0076-5392(99)x8001-5

6. A. A. Kilbas, H. M. Srivastava, J. J. Trujillo, *Theory and applications of fractional differential equations*, North-Holland Mathematics Studies, Amsterdam: Elsevier, 2006. https://doi.org/10.1016/S0304-0208(06)X8001-5

7. P. A. Naik, M. Yavuz, S. Qureshi, J. Zu, S. Townley, Modeling and analysis of COVID-19 epidemics with treatment in fractional derivatives using real data from Pakistan, *Eur. Phys. J. Plus*, **135** (2020), 795. https://doi.org/10.1140/epjp/s13360-020-00819-5

8. I. Ahmed, I. A. Baba, A. Yusuf, P. Kumam, W. Kumam, Analysis of Caputo fractional-order model for COVID-19 with lockdown, *Adv. Differ. Equ.*, **2020** (2020), 394. https://doi.org/10.1186/s13662-020-02853-0

9. M. Xiao, G. Jiang, J. Cao, W. Zheng, Local bifurcation analysis of a delayed fractional-order dynamic model of dual congestion control algorithms, *IEEE/CAA J. Autom. Sin.*, **4** (2017), 361–369. https://doi.org/10.1109/JAS.2016.7510151

10. G. Ilhem, M. Kouche, B. Ainseba, Stability analysis of a fractional-order SEIR epidemic model with general incidence rate and time delay, *Math. Methods Appl. Sci.*, **46** (2023), 10947–10969. https://doi.org/10.1002/mma.9161

11. X. Cui, D. Xue, F. Pan, Dynamic analysis and optimal control for a fractional-order delayed SIR epidemic model with saturated treatment, *Eur. Phys. J. Plus*, **137** (2022), 1–18. https://doi.org/10.1140/epjp/s13360-022-02810-8

12. C. Xu, Y. Yu, G. Ren, X. Si, Optimal control and bifurcation analysis of a delayed fractional-order epidemic model for the COVID-19 pandemic, *Int. J. Biomath.*, **18** (2025), 2450036. https://doi.org/10.1142/s1793524524500360

13. F. A. Rihan, Q. M. Al-Mdallal, H. J. AlSakaji, A. Hashish, A fractional-order epidemic model with time-delay and nonlinear incidence rate, *Chaos, Soliton. Fract.*, **126** (2019), 97–105. https://doi.org/10.1016/j.chaos.2019.05.039

14. R. Hu, M. H. N. Aziz, E. Aruchunan, N. A. Mohamed, Modeling and analysis of a delayed fractional order COVID-19 SEIHRM model with media coverage in Malaysia, *Sci. Rep.*, **15** (2025), 25305. https://doi.org/10.1038/s41598-025-99389-8

15. Y. Wang, J. Cao, M. Xiao, L. Zhao, Comprehensive bifurcation analysis in a delayed epidemic model with media coverage and asymptomatic infection via fractional PD control, *Nonlinear Ana.: Model. Control*, **31** (2026), 880–900. https://doi.org/10.15388/namc.2026.31.47299

16. C. Ma, Y. Zhao, X. Tan, Dynamic analysis of an infectious disease model with media coverage and saturated treatment, *Adv. Cont. Discr. Mod.*, **2026** (2026), 36. https://doi.org/10.1186/s13662-026-04073-4

17. T. Li, Y. Xiao, Complex dynamics of an epidemic model with saturated media coverage and recovery, *Nonlinear Dyn.*, **107** (2022), 2995–3023. https://doi.org/10.1007/s11071-021-07096-6

18. J. Mondal, S. Khajanchi, P. Samui, Impact of media awareness in mitigating the spread of an infectious disease with application to optimal control, *Eur. Phys. J. Plus*, **137** (2022), 983. https://doi.org/10.1140/epjp/s13360-022-03156-x

19. A. Recio-Román, M. Recio-Menéndez, M. V. Román-González, Influence of media information sources on vaccine uptake: the full and inconsistent mediating role of vaccine hesitancy, *Computation*, **11** (2023), 208. https://doi.org/10.3390/computation11100208

20. Y. Wang, F. Qing, H. Li, X. Wang, Timely and effective media coverage's role in the spread of Corona Virus Disease 2019, *Math. Methods Appl. Sci.*, **47** (2024), 3490–3506. https://doi.org/10.1002/mma.8732

21. X. Chang, J. Wang, M. Liu, Y. Yang, Stability analysis and optimal control of an epidemic model with multidimensional information of media coverage on networks, *Math. Methods Appl. Sci.*, **46** (2023), 6787–6802. https://doi.org/10.1002/mma.8940

22. S. Alahmadi, R. Hoyle, M. Head, M. Brede, Modelling the mitigation of anti-vaccine opinion propagation to suppress epidemic spread: a computational approach, *PLoS ONE*, **20** (2025), e0318544. https://doi.org/10.1371/journal.pone.0318544

23. W. Deng, C. Li, J. Lü, Stability analysis of linear fractional differential system with multiple time delays, *Nonlinear Dyn.*, **48** (2007), 409–416. https://doi.org/10.1007/s11071-006-9094-0

24. J. Cresson, A. Szafrańska, Discrete and continuous fractional persistence problems—the positivity property and applications, *Commun. Nonlinear Sci. Numer. Simul.*, **44** (2017), 424–448. https://doi.org/10.1016/j.cnsns.2016.07.016

25. H. L. Li, L. Zhang, C. Hu, Y. L. Jiang, Z. Teng, Dynamical analysis of a fractional-order predator-prey model incorporating a prey refuge, *J. Appl. Math. Comput.*, **54** (2017), 435–449. https://doi.org/10.1007/s12190-016-1017-8

26. T. A. Maraaba, F. Jarad, D. Baleanu, On the existence and the uniqueness theorem for fractional differential equations with bounded delay within Caputo derivatives, *Sci. China Ser. A: Math.*, **51** (2008), 1775–1786. https://doi.org/10.1007/s11425-008-0068-1

27. S. Bhalekar, V. Daftardar-Gejji, A predictor-corrector scheme for solving nonlinear delay differential equations of fractional order, *J. Fract. Calc. Appl.*, **1** (2011), 1–9.

Appendix

All coefficients listed in Appendices A.1 and A.2 were independently verified using the computer algebra system Maple.

A.1. Specific expressions of the coefficients d_i $(i = 0, \dots, 4)$*,* e_i $(i = 0, \dots, 3)$*,* f_i $(i = 1, 2)$ *in Eq* (4.22).

$$d_4 = -(a_{11} + a_{22} + a_{33} + a_{44} + a_{55});$$

$$d_3 = (a_{33} + a_{44} + a_{55} + a_{22})a_{11} + (a_{33} + a_{44} + a_{55})a_{22} + (a_{44} + a_{55})a_{33} - a_{32}a_{23} + a_{55}a_{44} - a_{21}a_{12} - a_{31}a_{13};$$

$$\begin{aligned} d_2 = {} & [(-a_{33} - a_{44} - a_{22})a_{11} + (-a_{33} - a_{22})a_{44} + a_{32}a_{23} - a_{33}a_{22} + a_{21}a_{12} + a_{31}a_{13}]a_{55} + [(-a_{33} - a_{22})a_{44} \\ & + a_{32}a_{23} - a_{33}a_{22}]a_{11} + (a_{12}a_{21} + a_{13}a_{31} - a_{22}a_{33} + a_{23}a_{32})a_{44} + a_{12}a_{21}a_{33} - a_{13}a_{21}a_{32} \end{aligned}$$

$$- a_{31}(a_{12}a_{23} - a_{13}a_{22});$$

$$\begin{aligned} d_1 = &\Big[(-a_{12}a_{33} - a_{12}a_{44} + a_{13}a_{32})a_{21} + (-a_{31}a_{13} + (a_{33} + a_{22})a_{11} - a_{32}a_{23} + a_{33}a_{22})a_{44} \\ &+ a_{31}(a_{12}a_{23} - a_{13}a_{22}) - a_{11}(-a_{22}a_{33} + a_{23}a_{32})\Big]a_{55} - \Big[(a_{12}a_{33} - a_{13}a_{32})a_{21} + (-a_{12}a_{23} \\ &+ a_{13}a_{22})a_{31} + a_{11}(-a_{22}a_{33} + a_{23}a_{32})\Big]a_{44}; \end{aligned}$$

$$d_0 = [(a_{12}a_{33} - a_{13}a_{32})a_{21} + (-a_{12}a_{23} + a_{13}a_{22})a_{31} + a_{11}(-a_{22}a_{33} + a_{23}a_{32})]a_{55}a_{44};$$

$$e_3 = -a_{42}b_{24} - a_{43}b_{34} - a_{52}b_{25};$$

$$\begin{aligned} e_2 = &(a_{42}b_{24} + a_{43}b_{34})a_{55} + (a_{42}b_{24} + a_{43}b_{34} + a_{52}b_{25})a_{11} + a_{44}a_{52}b_{25} + (a_{42}b_{24} + a_{52}b_{25})a_{33} + [(b_{24} + b_{34})a_{42} \\ &+ a_{52}(b_{25} + b_{35})]a_{21} + a_{43}b_{34}a_{22} + (-a_{42}b_{34} - a_{52}b_{35})a_{23} - [(-b_{24} - b_{34})a_{31} + a_{32}b_{24}]a_{43}; \end{aligned}$$

$$\begin{aligned} e_1 = &\Big[(-(b_{24} + b_{34})a_{42}a_{21} - a_{43}(b_{24} + b_{34})a_{31} + (-a_{42}b_{24} - a_{43}b_{34})a_{11} \\ &+ (-a_{22}b_{34} + a_{32}b_{24})a_{43} - a_{42}(-a_{23}b_{34} + a_{33}b_{24}))a_{55} + (-a_{52}(b_{25} + b_{35})a_{44} + (a_{32}b_{24} \\ &+ b_{34}(a_{32} + a_{12}))a_{43} + ((-b_{25} - b_{35})a_{33} - b_{35}a_{13})a_{52} - a_{42}((b_{24} + b_{34})a_{33} + b_{34}a_{13}))a_{21} \\ &- a_{52}(a_{11}b_{25} - a_{23}b_{35} + a_{33}b_{25})a_{44} + (((-a_{12} - a_{22})b_{24} - b_{34}a_{22})a_{43} + ((b_{25} + b_{35})a_{23} \\ &+ b_{25}a_{13})a_{52} + a_{42}((a_{13} + a_{23})b_{24} + b_{34}a_{23}))a_{31} + a_{11}((-a_{22}b_{34} + a_{32}b_{24})a_{43} \\ &+ (a_{23}b_{35} - a_{33}b_{25})a_{52} - a_{42}(-a_{23}b_{34} + a_{33}b_{24}))\Big]; \end{aligned}$$

$$\begin{aligned} e_0 = &\Big[\Big((-a_{32}b_{24} - b_{34}(a_{32} + a_{12}))a_{21} + ((a_{12} + a_{22})b_{24} + b_{34}a_{22})a_{31} - a_{11}(-a_{22}b_{34} + a_{32}b_{24})\Big)a_{43} \\ &+ a_{42}\Big((a_{33}b_{24} + b_{34}(a_{33} + a_{13}))a_{21} + ((-a_{13} - a_{23})b_{24} - b_{34}a_{23})a_{31} + a_{11}(-a_{23}b_{34} + a_{33}b_{24})\Big)\Big]a_{55} \\ &+ a_{52}a_{44}\Big(((b_{25} + b_{35})a_{33} + b_{35}a_{13})a_{21} + ((-b_{25} - b_{35})a_{23} - b_{25}a_{13})a_{31} + a_{11}(-a_{23}b_{35} + a_{33}b_{25})\Big); \end{aligned}$$

$$f_1 = -a_{43}a_{52}(b_{24}b_{35} - b_{25}b_{34}); \qquad f_0 = a_{43}a_{52}(a_{11} + a_{21} + a_{31})(b_{24}b_{35} - b_{25}b_{34}).$$

A.2. Specific expressions of the coefficients η_i $(i = 0, \ldots, 19)$ in Eq (4.27).

$$\eta_0 = (d_0 - f_0)^2(d_0 + e_0 + f_0)(d_0 - e_0 + f_0)$$

$$\eta_1 = 4\cos(\tfrac{1}{2}\alpha\pi)\Big(d_1d_0^2 + ((d_1 - f_1)f_0 - \tfrac{1}{2}e_0e_1)d_0 - f_0^2f_1 + \tfrac{1}{2}e_0e_1f_0 - \tfrac{1}{2}e_0^2(d_1 - f_1)\Big)(d_0 - f_0);$$

$$\begin{aligned} \eta_2 = &(4d_0^3d_2 + (2d_1^2 - 2e_0e_2)d_0^2 + (-2d_2e_0^2 + (-2d_1e_1 + 4e_2f_0)e_0 - 4d_2f_0^2 + (-4d_1f_1 + 2e_1^2)f_0)d_0 \\ &+ (2d_1f_1 + 2d_2f_0)e_0^2 + (-2e_1f_0f_1 - 2e_2f_0^2)e_0 + 2f_0^2f_1^2)\cos(\alpha\pi) \\ &+ (4d_1^2 - e_1^2 - 2f_1^2)d_0^2 + (-2e_1(d_1 - 2f_1)e_0 - 4d_1f_0f_1)d_0 + (-d_1^2 - f_1^2)e_0^2 \\ &+ 4(d_1 - \tfrac{1}{2}f_1)f_0e_1e_0 - 2f_0^2(d_1^2 + \tfrac{1}{2}e_1^2 - 2f_1^2); \end{aligned}$$

$$\begin{aligned} \eta_3 = &-16\cos(\tfrac{1}{2}\alpha\pi)\Big[\Big(-d_0^3d_3 + (-d_1d_2 + \tfrac{1}{2}e_0e_3)d_0^2 + (\tfrac{1}{2}d_3e_0^2 + (\tfrac{1}{2}d_1e_2 + \tfrac{1}{2}d_2e_1 - e_3f_0)e_0 + f_0(d_2f_1 + d_3f_0 - e_1e_2))d_0 \\ &+ \tfrac{1}{2}e_0(-(d_2f_1 + d_3f_0)e_0 + f_0(e_2f_1 + e_3f_0))\Big)\cos^2(\tfrac{1}{2}\alpha\pi) + \tfrac{3}{4}d_0^3d_3 + \tfrac{1}{4}(\tfrac{1}{2}e_1e_2 - \tfrac{3}{2}e_0e_3 + d_1d_2)d_0^2 \\ &+ \tfrac{1}{2}\Big(-\tfrac{3}{4}d_3e_0^2 + \tfrac{1}{2}(-d_1e_2 - d_2e_1 - e_2f_1 + 3e_3f_0)e_0 - \tfrac{3}{2}d_3f_0^2 + (\tfrac{3}{2}e_1e_2 - f_1d_2)f_0 \\ &+ \tfrac{1}{2}(d_1f_1 + d_1^2 - \tfrac{1}{2}e_1^2)(f_1 - d_1)\Big)d_0 + \tfrac{3}{8}(f_0d_3 + (\tfrac{1}{3}d_1 + f_1)d_2)e_0^2 \\ &+ \tfrac{1}{4}(-\tfrac{3}{2}e_3f_0^2 - (d_1e_2 + d_2e_1 + e_2f_1)f_0 + \tfrac{1}{2}e_1(f_1 - d_1)^2)e_0 \\ &+ \tfrac{1}{4}((\tfrac{1}{2}e_1e_2 + d_1d_2)f_0 - (f_1 - d_1)(f_1^2 + d_1f_1 - \tfrac{1}{2}e_1^2))f_0\Big]; \end{aligned}$$

$$\eta_4 = 16(2d_0^3d_4 + (2d_1d_3 + d_2^2)d_0^2 + (-d_4e_0^2 - (d_1e_3 + d_2e_2 + d_3e_1)e_0 + 2(e_1e_3 - f_0d_4 - f_1d_3 + \tfrac{1}{2}e_2^2)f_0)d_0$$

$$
\begin{aligned}
&- e_0(-(d_3 f_1 + d_4 f_0)e_0 + e_3 f_0 f_1)) \cos^4(\tfrac{1}{2}\alpha\pi)\\
&+ 4\Big(-8d_0^3 d_4 + (-4d_1 d_3 - 4d_2^2 - e_1 e_3)d_0^2 + (4d_4 e_0^2 + (3d_1 e_3 + 4d_2 e_2 + 3d_3 e_1 + 2e_3 f_1)e_0 + 8d_4 f_0^2\\
&+ 2(3d_3 f_1 - 4e_1 e_3 - 2e_2^2)f_0 - d_2 e_1^2 + 2e_2(f_1 - \tfrac{1}{2}d_1)e_1 - 2d_2(-2d_1^2 + f_1^2))d_0\\
&- 4(f_0 d_4 + (f_1 + \tfrac{1}{4}d_1)d_3)e_0^2 + ((2d_3 e_1 + 3(f_1 + \tfrac{2}{3}d_1)e_3)f_0 + 2(f_1 - \tfrac{1}{2}d_1)d_2 e_1 - e_2(d_1^2 + f_1^2))e_0\\
&- ((2d_1 d_3 + e_1 e_3)f_0 + e_2(f_1 - 2d_1)e_1 + 2f_1 d_1 d_2)f_0\Big) \cos^2(\tfrac{1}{2}\alpha\pi)\\
&+ 4d_0^3 d_4 + (-4d_1 d_3 + 6d_2^2 + 2e_1 e_3 - e_2^2)d_0^2\\
&+ 2(-d_4 e_0^2 - 2(d_2 e_2 + e_3 f_1)e_0 - 2d_4 f_0^2 + (2e_1 e_3 + e_2^2)f_0 + 2d_2 f_1^2 - 2e_1 e_2 f_1 - 2d_1^2 d_2 + d_2 e_1^2)d_0\\
&+ (2d_1 d_3 - d_2^2 + 2d_3 f_1 + 2d_4 f_0)e_0^2 + 2(2(-d_1 e_3 + d_2 e_2 - d_3 e_1)f_0 - 2f_1 d_2 e_1 + e_2(f_1 + d_1)^2)e_0\\
&+ (4d_1 d_3 - 2d_2^2 + 2e_1 e_3 - e_2^2)f_0^2 + 2(-2d_1 e_1 e_2 + d_2 e_1^2)f_0 + (f_1 - d_1)^2(f_1 + d_1 + e_1)(f_1 + d_1 - e_1);
\end{aligned}
$$

$$
\begin{aligned}
\eta_5 = &-2\Big[16\Big(-2d_0^3 - 2(d_1 d_4 + d_2 d_3)d_0^2 + (e_0^2 + (d_2 e_3 + d_3 e_2 + d_4 e_1)e_0 - 2f_0(-d_4 f_1 + e_2 e_3 - f_0))d_0 - e_0^2(d_4 f_1 + f_0)\Big) \cos^4(\tfrac{1}{2}\alpha\pi)\\
&+ 4\Big(10d_0^3 + 2(3d_1 d_4 + 5d_2 d_3)d_0^2 + (-5e_0^2 + (-5d_2 e_3 - 5d_3 e_2 - 4d_4 e_1)e_0 - 4d_1^2 d_3 + (-2d_2^2 + e_1 e_3)d_1\\
&- 10f_0^2 + 2(-4d_4 f_1 + 5e_2 e_3)f_0 + d_3 e_1^2 + (d_2 e_2 - 2e_3 f_1)e_1 + 2f_1^2 d_3 - e_2^2 f_1)d_0\\
&+ (d_1 d_4 + 5d_4 f_1 + 5f_0)e_0^2 + (e_3 d_1^2 + (d_2 e_2 + d_3 e_1)d_1 + e_3 f_1^2 - 2d_4 e_1 f_0 - 2f_1 d_3 e_1)e_0\\
&+ f_0((2d_3 f_1 + 2d_4 f_0 - 2e_1 e_3 - e_2^2)d_1 + e_3 f_1 e_1)\Big) \cos^2(\tfrac{1}{2}\alpha\pi)\\
&- 10d_0^3 + (2d_1 d_4 - 14d_2 d_3 + e_2 e_3)d_0^2 + (5e_0^2 + 2(3d_2 e_3 + 3d_3 e_2 + d_4 e_1)e_0 + 10d_1^2 d_3 + (2d_2^2 - 2e_1 e_3 + e_2^2)d_1\\
&+ 10f_0^2 + 2(2d_4 f_1 - 5e_2 e_3)f_0 - 3d_3 e_1^2 + 2(-d_2 e_2 + 3e_3 f_1)e_1 - 6f_1^2 d_3 + 3e_2^2 f_1)d_0\\
&+ (-3d_1 d_4 + d_2 d_3 - 5d_4 f_1 - 5f_0)e_0^2 + (-3e_3 d_1^2 - 2(d_2 e_2 + d_3 e_1 + e_3 f_1)d_1\\
&+ 2(-d_2 e_3 - d_3 e_2 + 3d_4 e_1)f_0 + (d_2^2 + 6d_3 f_1)e_1 - 3e_3 f_1^2 - 2d_2 e_2 f_1)e_0\\
&- 2d_1^3 d_2 + d_1^2 e_1 e_2 + (-6d_4 f_0^2 + (-4d_3 f_1 + 6e_1 e_3 + 3e_2^2)f_0 + 2d_2 f_1^2 - 2e_1 e_2 f_1 + d_2 e_1^2)d_1\\
&+ (2d_2 d_3 + e_2 e_3)f_0^2 + (-d_3 e_1^2 - 2(d_2 e_2 + e_3 f_1)e_1 + f_1(2d_2^2 + e_2^2))f_0 + f_1 e_1(-d_2 e_1 + e_2 f_1)\Big] \cos(\tfrac{1}{2}\alpha\pi);
\end{aligned}
$$

$$
\begin{aligned}
\eta_6 = &\ 64((2d_2 d_4 + d_3^2 + 2d_1)d_0^2 + (-(d_3 e_3 + d_4 e_2 + e_1)e_0 + f_0(e_3^2 - 2f_1))d_0 + e_0^2 f_1) \cos^6(\tfrac{1}{2}\alpha\pi)\\
&+ 16\Big(2(-6d_2 d_4 - 3d_3^2 - 4d_1)d_0^2 + (4d_1^2 d_4 + 4d_1 d_2 d_3 + (6d_3 e_3 + 6d_4 e_2 + 5e_1)e_0 - d_4 e_1^2\\
&- (d_2 e_3 + d_3 e_2)e_1 - 2f_1^2 d_4 + 2(e_2 e_3 + 5f_0)f_1 - 6e_3^2 f_0)d_0\\
&+ (-e_0^2 - (d_2 e_3 + d_3 e_2 + d_4 e_1)e_0 + 2f_0(-d_4 f_1 + e_2 e_3 - f_0))d_1 + 2(-3f_1 e_0 + e_1(d_4 f_1 + f_0))e_0\Big) \cos^4(\tfrac{1}{2}\alpha\pi)\\
&+ 4\Big((22d_2 d_4 + 9d_3^2 + 2d_1)d_0^2 + (-14d_1^2 d_4 + (-12d_2 d_3 - e_2 e_3)d_1 + (-9d_3 e_3 - 10d_4 e_2 - 5e_1)e_0\\
&+ 4d_4 e_1^2 + (4d_2 e_3 + 3d_3 e_2)e_1 + 8f_1^2 d_4 + 2(-4e_2 e_3 - 5f_0)f_1 + 9e_3^2 f_0 + 2d_2^3 - d_2 e_2^2)d_0\\
&+ 2d_1^3 d_3 + (d_2^2 - e_1 e_3)d_1^2 + (4e_0^2 + (3d_2 e_3 + 4d_3 e_2 + 3d_4 e_1)e_0 - d_3 e_1^2 + (-d_2 e_2 + 2e_3 f_1)e_1\\
&- 2f_1^2 d_3 + (6d_4 f_0 + e_2^2)f_1 - 8f_0(e_2 e_3 - f_0))d_1 + (-d_2 d_4 + 9f_1)e_0^2\\
&+ ((-d_2 d_3 - 8d_4 f_1 - 8f_0)e_1 + 2e_2(f_0 d_4 + f_1 d_3 - \tfrac{1}{2}d_2^2))e_0 + (d_3 f_1 + d_4 f_0)e_1^2\\
&+ e_3(2d_2 f_0 - f_1^2)e_1 - ((2d_2 d_3 + e_2 e_3)f_1 + d_2(2d_4 f_0 - e_2^2))f_0\Big) \cos^2(\tfrac{1}{2}\alpha\pi)\\
&+ (-12d_2 d_4 + 2d_3^2 - e_3^2 + 4d_1)d_0^2 + 2(2d_1^2 d_4 + 4d_1 d_2 d_3 - 2d_2^3 - 2d_2 e_1 e_3 + d_2 e_2^2\\
&+ 2d_4 e_0 e_2 - d_4 e_1^2 - 2d_4 f_1^2 + 2e_2 e_3 f_1 - e_3^2 f_0)d_0 - 4d_1^3 d_3 + (2d_2^2 + 2e_1 e_3 - e_2^2)d_1^2\\
&+ 2(-2d_3 e_0 e_2 + d_3 e_1^2 + 2d_3 f_1^2 - 2e_1 e_3 f_1 - e_2^2 f_1 + 2e_2 e_3 f_0 - e_0^2 - 2f_0^2)d_1\\
&+ (2d_2 d_4 - d_3^2 - 2f_1)e_0^2 + 2(2e_1(d_4 f_1 + f_0) + 2(d_2 e_3 - d_3 e_2)f_1 + d_2^2 e_2 + 2f_0(d_3 e_3 - d_4 e_2))e_0
\end{aligned}
$$

$$
\begin{aligned}
&+(-d_2^2-2d_3f_1-2d_4f_0)e_1^2+2(e_3f_1^2+2d_2e_2f_1-2f_0(d_2e_3-d_3e_2))e_1\\
&+(-2d_2^2-e_2^2)f_1^2+2(2d_4f_0^2-e_2^2f_0)d_2-f_0^2(2d_3^2+e_3^2);
\end{aligned}
$$

$$
\begin{aligned}
\eta_7 = -2\Big[&64(-2(d_3d_4+d_2)d_0+e_0(d_4e_3+e_2))d_0\cos^6(\tfrac{1}{2}\alpha\pi)\\
&+16\Big(14(d_3d_4+d_2)d_0^2+(-4d_1^2+2(-2d_2d_4-d_3^2)d_1-7e_0(d_4e_3+e_2)+d_4e_1e_2+e_1^2\\
&+e_3d_3e_1-f_1(e_3^2-2f_1))d_0+((d_3e_3+d_4e_2+e_1)e_0-f_0(e_3^2-2f_1))d_1-2e_0e_1f_1\Big)\cos^4(\tfrac{1}{2}\alpha\pi)\\
&+4\Big(4(-7d_3d_4-8d_2)d_0^2+(18d_1^2+2(8d_2d_4+5d_3^2)d_1-4d_2^2d_3+d_2e_2e_3+(14d_4e_3+15e_2)e_0\\
&-4d_4e_1e_2-5e_1^2-5e_3d_3e_1+d_3e_2^2+5f_1(e_3^2-2f_1))d_0-2d_1^3d_4-2d_1^2d_2d_3\\
&+(e_3d_2e_1+(-5d_3e_3-5d_4e_2-4e_1)e_0+(e_1^2+2f_1^2)d_4+d_3e_1e_2-2e_3f_1e_2\\
&+5f_0(e_3^2-\tfrac{8}{5}f_1))d_1+d_2^2e_0e_3+(e_0^2+(d_3e_2+d_4e_1)e_0-2f_0(-d_4f_1+e_2e_3-f_0))d_2\\
&+2(-d_4e_2f_1+5e_1f_1-e_2f_0)e_0-e_1^2(d_4f_1+f_0)\Big)\cos^2(\tfrac{1}{2}\alpha\pi)\\
&+2(5d_3d_4+13d_2)d_0^2+(-14d_1^2+(-12d_2d_4-14d_3^2+e_3^2)d_1+10d_2^2d_3-2d_2e_2e_3\\
&+2(-3d_4e_3-5e_2)e_0+2d_4e_1e_2+5e_1^2+6e_3d_3e_1-3d_3e_2^2-5f_1(e_3^2-2f_1))d_0\\
&+6d_1^3d_4+(2d_2d_3+e_2e_3)d_1^2+(-2d_2^3+(-2e_1e_3+e_2^2)d_2+2(3d_3e_3+3d_4e_2+e_1)e_0\\
&+3(-e_1^2-2f_1^2)d_4-2d_3e_1e_2+6e_3f_1e_2-5f_0(e_3^2-\tfrac{4}{5}f_1))d_1+(-3e_0e_3+e_1e_2)d_2^2\\
&+(-3e_0^2-2(d_3e_2+d_4e_1)e_0+6e_3f_0e_2-2e_3f_1e_1-4f_0f_1d_4+2f_1^2d_3-e_2^2f_1+d_3e_1^2-6f_0^2)d_2\\
&+d_3d_4e_0^2+(2(3e_2f_1-e_3f_0)d_4+(d_3^2-10f_1)e_1-2e_3f_1d_3+6f_0e_2)e_0\\
&+(2d_3f_0^2+3e_1^2f_1-2e_1e_2f_0)d_4+3e_1^2f_0-2d_3(e_2f_1+e_3f_0)e_1-d_3e_2^2f_0\\
&+e_2e_3f_1^2+f_0f_1(2d_3^2+e_3^2)\Big]\cos(\tfrac{1}{2}\alpha\pi);
\end{aligned}
$$

$$
\begin{aligned}
\eta_8 = &-256d_0(-d_0d_4^2-2d_0d_3+e_0e_3)\cos^8(\tfrac{1}{2}\alpha\pi)\\
&+64\Big(((4d_0d_3-e_0e_3)d_4+4d_0d_2-e_0e_2)d_1-d_0(8d_0d_4^2+d_4e_1e_3+16d_0d_3-8e_0e_3+e_1e_2)\Big)\cos^6(\tfrac{1}{2}\alpha\pi)\\
&+16\Big(2d_1^3+(2d_2d_4+d_3^2)d_1^2+((-24d_0d_3+6e_0e_3-e_1e_2)d_4+e_3^2f_1-e_3d_3e_1-2f_1^2\\
&-20d_0d_2+6e_0e_2-e_1^2)d_1+20d_0^2d_4^2+((4d_2^2+6e_1e_3-e_2^2)d_0-d_2e_0e_2)d_4+40d_0^2d_3\\
&+(2d_2d_3^2-d_3e_2e_3-20e_0e_3+5e_1e_2)d_0+(-d_3e_0e_3+e_3^2f_0-e_0e_1-2f_0f_1)d_2+2f_1(e_0e_2+\tfrac{1}{2}e_1^2)\Big)\cos^4(\tfrac{1}{2}\alpha\pi)\\
&+4\Big(-8d_1^3-4(d_2d_4+d_3^2)d_1^2+((40d_0d_3-9e_0e_3+3e_1e_2)d_4+24d_0d_2+4d_2^2d_3-d_2e_2e_3\\
&+(4e_1e_3-e_2^2)d_3-4e_3^2f_1+8f_1^2-10e_0e_2+4e_1^2)d_1-16d_0^2d_4^2+(2(-8d_2^2-5e_1e_3+2e_2^2)d_0\\
&+(4e_0e_2-e_1^2-2f_1^2)d_2+(-e_0e_1-2f_0f_1)d_3+2(e_0e_3+e_1e_2)f_1)d_4-28d_0^2d_3\\
&+((-4d_3^2-e_3^2)d_2+3e_3d_3e_2+15e_0e_3-5e_1e_2)d_0-d_2^2e_1e_3+((3e_0e_3-e_1e_2)d_3-4e_3^2f_0+2e_3f_1e_2\\
&+6f_0f_1+3e_0e_1)d_2-d_3^2e_0e_2+(2e_2e_3f_0-e_0^2-2f_0^2)d_3+2e_0e_3f_0\\
&+2(-4e_0f_1+e_1f_0)e_2-4e_1^2f_1\Big)\cos^2(\tfrac{1}{2}\alpha\pi)\\
&+4d_1^3+(-4d_2d_4+6d_3^2-e_3^2)d_1^2+2(-4d_0d_3d_4-4d_0d_2-2d_2^2d_3+(-2e_1e_3+e_2^2)d_3+e_3^2f_1-2f_1^2\\
&+2e_0e_2-e_1^2)d_1+(6d_0^2-e_0^2-2f_0^2)d_4^2+2((6d_2^2+2e_1e_3-e_2^2)d_0+(-2e_0e_2+e_1^2+2f_1^2)d_2\\
&+2(-e_0f_1+e_1f_0)e_3+f_0e_2^2-2e_1e_2f_1)d_4-4d_0^2d_3+2d_2(-2d_3^2+e_3^2)d_0\\
&+d_2^4+(2e_1e_3-e_2^2)d_2^2+2(-2e_2e_3f_1+e_3^2f_0)d_2+(2e_0e_2-e_1^2-2f_1^2)d_3^2\\
&+2(2(e_1f_1-e_2f_0)e_3+e_2^2f_1+2f_0^2+e_0^2)d_3-e_3^2f_1^2-4e_0e_3f_0+4(e_0f_1-e_1f_0)e_2+2e_1^2f_1;
\end{aligned}
$$

$$
\begin{aligned}
\eta_9 = 8\Big[&128\cos^8(\tfrac{1}{2}\alpha\pi)d_0^2d_4 + 16\Big(2d_0d_1d_4^2 - 18d_0^2d_4 - (d_0e_1 + d_1e_0)e_3 + 4d_0d_1d_3\Big)\cos^6(\tfrac{1}{2}\alpha\pi) \\
&+ 4\Big(-14d_0d_1d_4^2 + (-(d_0e_2 + d_1e_1 + d_2e_0)e_3 + 2(2d_0d_2 + d_1^2)d_3 + 54d_0^2)d_4 \\
&+ 7(d_0e_1 + d_1e_0)e_3 - 28d_0d_1d_3 + (4d_2^2 - e_2^2)d_0 + 2d_1^2d_2 - d_1e_1e_2 - d_2e_0e_2\Big)\cos^4(\tfrac{1}{2}\alpha\pi) \\
&+ \Big(28d_0d_1d_4^2 + ((4d_0e_2 + 5d_1e_1 + 5d_2e_0)e_3 + (-16d_0d_2 - 10d_1^2 - e_0e_2)d_3 - 60d_0^2 \\
&+ (4d_2^2 - e_2^2)d_1 - d_2e_1e_2)d_4 + ((f_0 - d_0)d_3 + f_1d_2)e_3^2 + (-d_3^2e_0 - (d_1e_2 + d_2e_1)d_3 - 15d_0e_1 + 2e_0(f_1 - 7d_1))e_3 \\
&+ 2d_0d_3^3 + 2d_1d_2d_3^2 + (60d_0d_1 - e_0e_1 - 2f_0f_1)d_3 + 5(-4d_2^2 + e_2^2)d_0 - 6d_1^2d_2 + 4d_1e_1e_2 \\
&+ (5e_0e_2 - e_1^2 - 2f_1^2)d_2 + 2e_1e_2f_1\Big)\cos^2(\tfrac{1}{2}\alpha\pi) \\
&+ \tfrac{1}{2}(-5d_0d_1 - f_0f_1 - \tfrac{1}{2}e_0e_1)d_4^2 + \Big(\tfrac{1}{2}(-d_0e_2 - 3d_1e_1 - 3d_2e_0 + e_1f_1 + e_2f_0)e_3 \\
&+ (\tfrac{7}{2}d_1^2 - \tfrac{1}{2}f_1^2 - \tfrac{1}{4}e_1^2 + 3d_0d_2 + \tfrac{1}{2}e_0e_2)d_3 + \tfrac{11}{2}d_0^2 + \tfrac{1}{2}(\tfrac{3}{2}e_2^2 - 5d_2^2)d_1 - \tfrac{1}{2}f_0^2 - \tfrac{1}{4}e_0^2 \\
&+ \tfrac{1}{4}e_2^2f_1 + \tfrac{1}{2}d_2e_1e_2\Big)d_4 + \tfrac{3}{4}((d_0 - f_0)d_3 - (\tfrac{1}{3}d_1 + f_1)d_2)e_3^2 \\
&+ \tfrac{1}{2}\Big(\tfrac{3}{2}d_3^2e_0 + (d_1e_2 + d_2e_1 + e_2f_1)d_3 - 3f_1e_0 + 5d_0e_1 + e_1f_0 + 3d_1e_0 - \tfrac{1}{2}d_2^2e_2\Big)e_3 \\
&- \tfrac{3}{2}d_0d_3^3 + \tfrac{1}{2}(-d_1d_2 - \tfrac{1}{2}e_1e_2)d_3^2 + (\tfrac{1}{2}e_0e_1 + f_0f_1 + \tfrac{1}{2}d_2^3 - 9d_0d_1 - \tfrac{1}{4}d_2e_2^2)d_3 \\
&+ \tfrac{1}{2}(11d_2^2 - \tfrac{5}{2}e_2^2)d_0 - \tfrac{1}{2}d_1^2d_2 - \tfrac{1}{2}d_1e_1e_2 + \tfrac{3}{2}(f_1^2 - e_0e_2 + \tfrac{1}{2}e_1^2)d_2 + \tfrac{1}{4}e_2(-6e_1f_1 + e_2f_0)\Big]\cos(\tfrac{1}{2}\alpha\pi);
\end{aligned}
$$

$$
\begin{aligned}
\eta_{10} = &1024d_0^2\cos^{10}(\tfrac{1}{2}\alpha\pi) + 512(2d_0d_1d_4 - 5d_0^2)\cos^8(\tfrac{1}{2}\alpha\pi) \\
&+ 64\Big((2d_0d_2 + d_1^2)d_4^2 - 32d_0d_1d_4 + 2(2d_0d_2 + d_1^2)d_3 - (d_0e_2 + d_1e_1 + d_2e_0)e_3 + 35d_0^2\Big)\cos^6(\tfrac{1}{2}\alpha\pi) \\
&+ 16\Big(6(-2d_0d_2 - d_1^2)d_4^2 + (4d_0d_3^2 + (4d_1d_2 - e_0e_3)d_3 - e_3^2d_0 - (d_1e_2 + d_2e_1)e_3 + 80d_0d_1)d_4 \\
&+ (-20d_0d_2 - 12d_1^2 - e_0e_2)d_3 + (5d_0e_2 + 6d_1e_1 + 6d_2e_0)e_3 + (4d_2^2 - e_2^2)d_1 - d_2e_1e_2 - 50d_0^2\Big)\cos^4(\tfrac{1}{2}\alpha\pi) \\
&+ 4\Big((22d_0d_2 + 9d_1^2 - e_0e_2)d_4^2 + (-14d_0d_3^2 + (-12d_1d_2 + 3e_0e_3 - e_1e_2)d_3 + (f_0 + 4d_0)e_3^2 \\
&+ (3d_1e_2 + 4d_2e_1)e_3 + 2d_2^3 - d_2e_2^2 - 2f_0f_1 - 60d_0d_1 - e_0e_1)d_4 + 2d_1d_3^3 + (d_2^2 - e_1e_3)d_3^2 \\
&+ ((f_1 - d_1)e_3^2 - d_2e_2e_3 - 2f_1^2 + 20d_0d_2 + 22d_1^2 + 4e_0e_2 - e_1^2)d_3 \\
&+ (-5d_0e_2 - 10d_1e_1 - 9d_2e_0 + 2e_1f_1)e_3 + 2(-7d_2^2 + 2e_2^2)d_1 + e_2^2f_1 + 3d_2e_1e_2 + 25d_0^2\Big)\cos^2(\tfrac{1}{2}\alpha\pi) \\
&+ (-12d_0d_2 + 2d_1^2 + 2e_0e_2 - e_1^2 - 2f_1^2)d_4^2 + 2(2d_0d_3^2 + 4d_1d_2d_3 - (f_0 + d_0)e_3^2 + 2(-d_2e_1 + e_2f_1)e_3 \\
&- 2d_2^3 + d_2e_2^2 + 4d_0d_1)d_4 - 4d_1d_3^3 + (2d_2^2 + 2e_1e_3 - e_2^2)d_3^2 \\
&+ 2((d_1 - f_1)e_3^2 + 2f_1^2 + 4d_0d_2 - 6d_1^2 - 2e_0e_2 + e_1^2)d_3 - d_2^2e_3^2 + 4(d_1e_1 - e_1f_1 + e_2f_0)e_3 \\
&+ 2(2d_2^2 - e_2^2)d_1 - 2e_2^2f_1 - 2f_0^2 + 2d_0^2 - e_0^2;
\end{aligned}
$$

$$
\begin{aligned}
\eta_{11} = 2\Big[&512\cos^8(\tfrac{1}{2}\alpha\pi)d_0d_1 + 128((2d_0d_2 + d_1^2)d_4 - 9d_0d_1)\cos^6(\tfrac{1}{2}\alpha\pi) \\
&+ 16\Big(2(d_0d_3 + d_1d_2)d_4^2 + 14(-2d_0d_2 - d_1^2)d_4 - e_3^2d_0 - (d_1e_2 + d_2e_1 + d_3e_0)e_3 + 4d_0d_3^2 + 4d_1d_2d_3 + 54d_0d_1\Big)\cos^4(\tfrac{1}{2}\alpha\pi) \\
&+ 4\Big((-6d_0d_3 - 10d_1d_2 - e_0e_3)d_4^2 + (-e_3^2d_1 - (d_2e_2 + d_3e_1)e_3 + 4d_1d_3^2 + 2d_2^2d_3 + 60d_0d_2 + 28d_1^2 - e_0e_2)d_4 \\
&+ 5e_3^2d_0 + (4d_1e_2 + 5d_2e_1 + 5d_3e_0)e_3 - 20d_0d_3^2 + (-16d_1d_2 - e_1e_2)d_3 + 2d_2^3 - d_2e_2^2 - 60d_0d_1\Big)\cos^2(\tfrac{1}{2}\alpha\pi) \\
&+ (-2d_0d_3 + 14d_1d_2 + 3e_0e_3 - e_1e_2)d_4^2 + ((f_1 + 3d_1)e_3^2 + 2(d_2e_2 + d_3e_1)e_3 - 10d_1d_3^2 + (-2d_2^2 - e_2^2)d_3 \\
&- 2f_1^2 - 36d_0d_2 - 10d_1^2 + 2e_0e_2 - e_1^2)d_4 + (-d_2d_3 - 5d_0 + f_0)e_3^2 \\
&+ (-d_3^2e_2 - 6d_3e_0 - 6d_2e_1 + 2e_2(f_1 - d_1))e_3 + 2d_2d_3^3 + 22d_0d_3^2 + 2(6d_1d_2 + e_1e_2)d_3 - 6d_2^3 + 3d_2e_2^2 \\
&- 2f_0f_1 + 22d_0d_1 - e_0e_1\Big]\cos(\tfrac{1}{2}\alpha\pi);
\end{aligned}
$$

$$
\begin{aligned}
\eta_{12} = {}& 256(2d_0d_2 + d_1^2)\cos^8(\tfrac{1}{2}\alpha\pi) + 256((d_0d_3 + d_1d_2)d_4 - 4d_0d_2 - 2d_1^2)\cos^6(\tfrac{1}{2}\alpha\pi)\\
& + 16\Big(2d_0d_4^3 + (2d_1d_3 + d_2^2)d_4^2 + (-20d_0d_3 - 24d_1d_2 - e_0e_3)d_4 + 4d_1d_3^2 + (2d_2^2 - e_1e_3)d_3\\
& + (-e_2e_3 + 40d_0)d_2 - d_1(e_3^2 - 20d_1)\Big)\cos^4(\tfrac{1}{2}\alpha\pi)\\
& + 4\Big(-8d_0d_4^3 + (-4d_1d_3 - 4d_2^2 - e_1e_3)d_4^2 + (4d_2d_3^2 + (-e_2e_3 + 24d_0)d_3 + (-e_3^2 + 40d_1)d_2 + 3e_0e_3 - e_1e_2)d_4\\
& - 16d_1d_3^2 + (-4d_2^2 + 4e_1e_3 - e_2^2)d_3 + (3e_2e_3 - 28d_0)d_2 + 4e_3^2d_1 - 16d_1^2 - e_0e_2\Big)\cos^2(\tfrac{1}{2}\alpha\pi)\\
& + 4d_0d_4^3 + (-4d_1d_3 + 6d_2^2 + 2e_1e_3 - e_2^2)d_4^2 + 2(-2d_2d_3^2 - 4d_0d_3 + d_2(e_3^2 - 4d_1))d_4 + d_3^4 + (-e_3^2 + 12d_1)d_3^2\\
& + 2(-2d_2^2 - 2e_1e_3 + e_2^2)d_3 + 2e_3^2f_1 - 2e_3^2d_1 - 2f_1^2 - 4d_0d_2 + 6d_1^2 + 2e_0e_2 - e_1^2;
\end{aligned}
$$

$$
\begin{aligned}
\eta_{13} = {}& -8\cos(\tfrac{1}{2}\alpha\pi)\Big[-32(d_0d_3 + d_1d_2)\cos^6(\tfrac{1}{2}\alpha\pi) + 8(-2d_0d_4^2 + (-2d_1d_3 - d_2^2)d_4 + 7d_0d_3 + 7d_1d_2)\cos^4(\tfrac{1}{2}\alpha\pi)\\
& + \Big(-2d_1d_4^3 + 2(-d_2d_3 + 9d_0)d_4^2 + (16d_1d_3 + 10d_2^2 + e_1e_3)d_4 - 4d_2d_3^2 + (e_2e_3 - 32d_0)d_3\\
& + (e_3^2 - 28d_1)d_2 + e_0e_3\Big)\cos^2(\tfrac{1}{2}\alpha\pi) + \tfrac{3}{2}d_1d_4^3 + \tfrac{1}{2}(\tfrac{1}{2}e_2e_3 + d_2d_3 - 7d_0)d_4^2\\
& + (-\tfrac{1}{2}d_3^3 + (\tfrac{1}{4}e_3^2 - 3d_1)d_3 - \tfrac{1}{2}e_1e_3 + \tfrac{1}{4}e_2^2 - \tfrac{7}{2}d_2^2)d_4 + \tfrac{5}{2}d_2d_3^2 + \tfrac{1}{2}(-e_2e_3 + 13d_0)d_3\\
& + \tfrac{1}{2}(-\tfrac{3}{2}e_3^2 + 5d_1)d_2 + \tfrac{1}{4}e_1e_2 - \tfrac{3}{4}e_0e_3\Big];
\end{aligned}
$$

$$
\begin{aligned}
\eta_{14} = {}& 64(2d_0d_4 + 2d_1d_3 + d_2^2)\cos^6(\tfrac{1}{2}\alpha\pi) + 32(2d_1d_4^2 + 2(d_2d_3 - 2d_0)d_4 - 6d_1d_3 - 3d_2^2)\cos^4(\tfrac{1}{2}\alpha\pi)\\
& + 4\Big(2d_2d_4^3 + (d_3^2 - 14d_1)d_4^2 + (-12d_2d_3 - e_2e_3 + 2d_0)d_4 + 2d_3^3 + (-e_3^2 + 22d_1)d_3 + 9d_2^2 - e_1e_3\Big)\cos^2(\tfrac{1}{2}\alpha\pi)\\
& - 4d_2d_4^3 + (2d_3^2 - e_3^2 + 4d_1)d_4^2 + 4(2d_2d_3 + d_0)d_4 - 4d_3^3 + 2(e_3^2 - 6d_1)d_3 + 2d_2^2 + 2e_1e_3 - e_2^2;
\end{aligned}
$$

$$
\begin{aligned}
\eta_{15} = {}& 64\Big((d_1d_4 + d_2d_3 + d_0)\cos^4(\tfrac{1}{2}\alpha\pi) + \tfrac{1}{2}(d_2d_4^2 + \tfrac{1}{2}(d_3^2 - 3d_1)d_4 - \tfrac{5}{2}d_2d_3 - \tfrac{5}{2}d_0)\cos^2(\tfrac{1}{2}\alpha\pi)\\
& + \tfrac{1}{16}d_3d_4^3 - \tfrac{5}{16}d_2d_4^2 + \tfrac{1}{16}(-d_3^2 - \tfrac{1}{2}e_3^2 - d_1)d_4 + \tfrac{7}{16}d_2d_3 - \tfrac{1}{32}e_2e_3 + \tfrac{5}{16}d_0\Big)\cos(\tfrac{1}{2}\alpha\pi);
\end{aligned}
$$

$$
\begin{aligned}
\eta_{16} = {}& 16(2d_2d_4 + d_3^2 + 2d_1)\cos^4(\tfrac{1}{2}\alpha\pi) + 16(d_3d_4^2 - d_2d_4 - d_3^2 - 2d_1)\cos^2(\tfrac{1}{2}\alpha\pi)\\
& + d_4^4 - 4d_3d_4^2 - 4d_2d_4 + 6d_3^2 - e_3^2 + 4d_1;
\end{aligned}
$$

$$\eta_{17} = 16(d_3d_4 + d_2)\cos^3(\tfrac{1}{2}\alpha\pi) + 4(d_4^3 - d_3d_4 - 3d_2)\cos(\tfrac{1}{2}\alpha\pi);$$

$$\eta_{18} = (2d_4^2 + 4d_3)\cos(\alpha\pi) + 4d_4^2; \qquad \eta_{19} = 4d_4\cos(\tfrac{1}{2}\alpha\pi).$$